Fungal Genetics and Biology 75 (2015) 30–45

Contents lists available at ScienceDirect

Fungal Genetics and Biology

journal homepage: www.elsevier.com/locate/yfgbi

Dissecting the function of the different chitin synthases in vegetative growth and sexual development in *Neurospora crassa*

Rosa A. Fajardo-Somera [a,1], Bastian Jöhnk [b], Özgür Bayram [b,2], Oliver Valerius [b], Gerhard H. Braus [b], Meritxell Riquelme [a,*]

[a] Department of Microbiology, Center for Scientific Research and Higher Education of Ensenada, CICESE, Ctra. Ensenada-Tijuana No. 3918, Ensenada, Baja California C.P. 22860, Mexico
[b] Department of Molecular Microbiology and Genetics, Georg-August Universität Göttingen, Grisebachstrasse 8, 37077 Göttingen, Germany

ARTICLE INFO

Article history:
Received 30 September 2014
Accepted 7 January 2015
Available online 13 January 2015

Keywords:
Cell wall
Chitin synthase
Hyphal morphogenesis
Proteomics
Sexual development
Spitzenkörper

ABSTRACT

Chitin, one of the most important carbohydrates of the fungal cell wall, is synthesized by chitin synthases (CHS). Seven sequences encoding CHSs have been identified in the genome of *Neurospora crassa*. Previously, CHS-1, -3 and -6 were found at the Spitzenkörper (Spk) core and developing septa. We investigated the functional importance of each CHS in growth and development of *N. crassa*. The cellular distribution of each CHS tagged with fluorescent proteins and the impact of corresponding gene deletions on vegetative growth and sexual development were compared. CHS-2, -4, -5 and -7 were also found at the core of the Spk and in forming septa in vegetative hyphae. As the septum ring developed, CHS-2-GFP remained at the growing edge of the septum until it localized around the septal pore. In addition, all CHSs were located in cross-walls of conidiophores. A partial co-localization of CHS-1-m and CHS-5-GFP or CHS-2-GFP occurred in the Spk and septa. Analyses of deletion mutants suggested that CHS-6 has a role primarily in hyphal extension and ascospore formation, CHS-5 in aerial hyphae, conidia and ascospore formation, CHS-3 in perithecia development and CHS-7 in all of the aforementioned. We show that *chs-7*/*csmB* fulfills a sexual function and *chs-6*/*chsG* fulfills a vegetative growth function in *N. crassa* but not in *Aspergillus nidulans*, whereas vice versa *chs-2*/*chsA* fulfills a sexual function in *A. nidulans* but not in *N. crassa*. This suggests that different classes of CHSs can fulfill distinct developmental functions in various fungi. Immunoprecipitation followed by mass spectrometry of CHS-1-GFP, CHS-4-GFP and CHS-5-GFP identified distinct putative interacting proteins for each CHS. Collectively, our results suggest that there are distinct populations of chitosomes, each carrying specific CHSs, with particular roles during different developmental stages.

1. Introduction

The cell wall is a structure, which gives support and protection to the fungal cell, and maintains osmotic pressure (Gooday, 1994). The main structural components of the fungal cell wall are β-(1,3)-glucan and chitin. Chitin is a linear homopolymer of β-(1-4)-linked *N*-acetylglucosamine (Cid et al., 1995; Sentandreu et al., 1984). The amount of chitin in the cell wall is variable, depending on the fungal species and the developmental stage (Bartnicki-García and Reyes, 1968; Braun and Calderone, 1978; Wessels, 1986). In the cell wall of the budding yeast *Saccharomyces cerevisiae*, chitin constitutes only about 1% of the total polysaccharide content, whereas significantly higher chitin contents of up to 40% have been described for filamentous fungi (Bartnicki-García and Nickerson, 1962; Cassone, 1986; Hearn and Sietsma, 1994). Chitin synthesis is catalyzed by enzymes of the family of chitin synthases (CHS) (Glaser and Brown, 1957), which mediate the transfer of *N*-acetylglucosamine to a growing chitin chain. CHSs are proteins with four to seven transmembrane domains. The genomes of filamentous fungi contain more than 10 CHS-encoding sequences, whereas yeast genomes contain three to four CHS-encoding genes. According to their amino acid sequences, CHSs are classified into seven classes (Choquer et al., 2004; Mandel et al., 2006; Riquelme and Bartnicki-García, 2008; Sheng et al., 2013), which are grouped in three divisions (Riquelme and Bartnicki-García, 2008). Division I CHSs, which includes CHSs classes I, II and III, are characterized by having a hydrophobic C-terminus and a conserved catalytic

* Corresponding author.
E-mail address: riquelme@cicese.mx (M. Riquelme).
[1] Present address: Karlsruhe Institute of Technology (KIT) – South Campus, Institute for Applied Biosciences, Department of Microbiology, Hertzstrasse 16, D-76187 Karlsruhe, Germany.
[2] Present address: Department of Biology, National University of Ireland Maynooth, Maynooth, Co. Kildare, Ireland.

http://dx.doi.org/10.1016/j.fgb.2015.01.002
1087-1845/

subdomain surrounded by a hydrophilic N-terminus region; division II contains CHSs classes IV, V and VII, which typically have a catalytic domain preceded by a cytochrome b5-binding type domain (pfam00173); and division III consists of class VI CHSs, with no domain other than the pfam03142 shared by all CHSs (Choquer et al., 2004; Riquelme and Bartnicki-García, 2008; Sheng et al., 2013).

The three classes of CHSs in *S. cerevisiae* have a specific role during cell growth and development (Bulawa, 1992; Bulawa et al., 1986; Silverman et al., 1988; Valdivieso et al., 1991). Chs3p (class IV) has the most important role in chitin synthesis, since it synthesizes around 90% of the chitin in the cell wall (Shaw et al., 1991; Valdivieso et al., 1991). Single mutants for each CHS are viable in *S. cerevisiae*, while double mutants for Chs1p (class 1) and Chs2p (class II) are unviable (Bulawa et al., 1986; Cid et al., 1995). In the dimorphic fungus *Candida albicans* four *CHS*s encoding sequences have been described (Bulawa et al., 1995; Gow et al., 1994). CaChs2 (class II) is involved in synthesizing chitin in the hyphal form (Gow et al., 1994); CaChs1 (class I) participates in septum formation in both yeast and filamentous forms (Munro et al., 2001), and CaChs3 (class IV) produces the majority of chitin in both yeast and filamentous forms (Bulawa et al., 1995; Mio et al., 1996). Finally, CaChs8 (class II) does not seem to have any important role during growth in both yeast and hyphal forms (Munro et al., 2003).

In the filamentous fungi *Aspergillus nidulans*, *Aspergillus fumigatus*, *Ustilago maydis*, *Fusarium oxysporum*, and *Botrytis cinerea*, different roles for each class of CHS have been described. In *A. nidulans* and *A. fumigatus*, class I CHS mutants *chsC* and *chsA*, respectively, displayed normal phenotype when compared to WT strains (Motoyama et al., 1994; Rogg et al., 2011). However, in other fungal species class I CHSs seem to have an important role. For instance, in *B. cinerea chs1* is involved in hyphal growth and pathogenicity (Soulie et al., 2006; Wang et al., 2001). Class II CHSs do not have an essential role in filamentous fungi. Mutations of *chsA* in *A. nidulans*, *chs2* in *U. maydis*, and *chs-2*^{rip} in *N. crassa* did not show any important phenotype (Din and Yarden, 1994; Motoyama et al., 1997; Weber et al., 2006). Class III CHSs are apparently quite important in *A. nidulans*, *A. fumigatus* and *B. cinerea*; each of the three species has two class III CHSs (Fukuda et al., 2009; Mellado et al., 1996; Soulie et al., 2006). Deletion of *chsG* in *A. fumigatus* caused a decrease in colony growth and chitin synthase activity, whereas deletion of *chsC* did not have any evident effect (Mellado et al., 1996). *N. crassa chs-1*^{rip} mutants yielded abnormally swollen and slow growing hyphae (Yarden and Yanofsky, 1991), although a Δ*chs-1* strain did not display any obvious defective phenotype (Sánchez-León et al., 2011). In *B. cinerea* while Chs3a participated in virulence and growth, Chs3b, did not have any role during both processes (Arbelet et al., 2010; Soulie et al., 2006). Class IV CHSs are not crucial for growth or morphology in *A. nidulans* (*chsD*) or *N. crassa* (*chs-4*^{rip}) (Din et al., 1996; Motoyama et al., 1996; Specht et al., 1996); whereas in *U. maydis*, Chs5 and Chs7 have important roles for fungal morphogenesis (Weber et al., 2006; Xoconostle-Cazares et al., 1997). CHSs classes V and VII contain a N-terminal myosin motor-like domain (MMD), which is essential for apical growth and morphogenesis in *A. nidulans* (*csmA* and *csmB*), *Colletrotrichum graminicola* (*ChsVb*), *Fusarium verticilliodes* (*CHS5* and *CHS7*), *A. fumigatus* (*chsE*), and *U. maydis* (*Msc1*) (Amnuaykanjanasin and Epstein, 2003, 2006; Larson et al., 2011; Mellado et al., 2003; Takeshita et al., 2002, 2005, 2006; Weber et al., 2006). The latest identified class VI CHSs have not been investigated in great detail. *N. crassa chs-6* knockout mutant showed a drastic reduction in growth rate (Sánchez-León et al., 2011). To identify the role of each CHS during the different developmental stages, we investigated the localization of each CHS tagged with fluorescent proteins in *N. crassa* and the effects of corresponding gene deletions.

2. Material and methods

2.1. Strains and culture conditions

N. crassa single mutants Δ*chs-1*, Δ*chs-2*, Δ*chs-3*, Δ*chs-4*, Δ*chs-5*, Δ*chs-6*, and Δ*chs-7* were generated by the Neurospora genome project and obtained from the Fungal Genetics Stock Center (Table 1). All strains except Δ*chs-1* and Δ*chs-4*, which contained also a copy of the native gene, were confirmed to be homokaryons with the corresponding *chs* gene deleted. Therefore, all the subsequent analyses were conducted on strains Δ*chs-2*, Δ*chs-3*, Δ*chs-5*, Δ*chs-6*, and Δ*chs-7*. For growth, branching and septation analysis, 5×10^4 conidia for each corresponding strain were inoculated onto Vogel's minimum medium agar plates (VMM; Vogel, 1956) and incubated at 30 °C for 24 h. For aerial hyphae and conidiation analyses, 5×10^4 conidia were inoculated into borosilicate tubes containing 2 ml of VMM agar and incubated at 30 °C during 5 days. For biomass experiments, 1×10^4 conidia were inoculated into test tubes containing 5 ml of liquid VMM and incubated at 30 °C for 48 h at 200 rpm; mycelium was harvested, washed with distilled water and dried for 16 h at 60 °C. For crosses, strains of each mating type were grown on synthetic crossing medium during 30 days at 25 °C (Westergaard and Mitchell, 1947).

Transformed conidia were spread directly onto plates containing FGS medium [0.05% (w/v) Fructose, 0.05% (w/v) Glucose, 2% (w/v) Sorbose] or mixed with Top-Agar (1× Vogel's salts, 1 M sorbitol, 1% agar, 1× FGS) and spread onto plates containing FGS medium supplemented with hygromycin (300 μg/ml; Roche). For confocal microscopy, transformants of *N. crassa* expressing GFP or mChFP were routinely grown on VMM overnight at 30 °C. For imaging, the "inverted agar block method" was used as previously described (Hickey et al., 2004). Strains used or generated in this study are listed in Table 1.

The *A. nidulans* strain AGB551 (Bayram et al., 2012) was used for the deletion of *chs* genes. *Aspergillus* strains were grown on minimal medium [1% D-glucose, 1× AspA (70 mM $NaNO_3$, 7 mM KCl, 11.2 mM KH_2PO_4, pH 5.5), 2 mM $MgSO_4$, 1× trace elements (76 μM $ZnSO_4$, 178 μM H_3BO_3, 25 μM $MnCl_2$, 18 μM $FeSO_4$, 7.1 μM $CoCl_2$, 6.4 μM $CuSO_4$, 6.2 μM Na_2MoO_4, 174 μM EDTA)] (Bennett and Lasure, 1991), supplemented with 100 μM pyridoxine–HCl, 10 mM uracil and 1 mM uridine at 37 °C. Solid media consisted of 2% (w/v) agar. For selective medium 100 ng ml^{-1} pyrithiamine were added. Vegetative cultures were grown in liquid submerged medium. Sexual development of WT and the mutant strains was promoted on minimal media plates in darkness with limited oxygen supply, for at least 6 days.

2.2. Molecular techniques

To fluorescently tag CHS proteins (*chs-2*, NCU05239; *chs-4*, NCU09324; *chs-5*, NCU04352; *chs-7*, NCU04350), we constructed strains in which the 3′ end of the ORF of the *chs* gene at its chromosomic location was fused to the *gfp* gene, using fusion PCR as described previously (Riquelme et al., 2014). Primer pairs P1–P2 and P3–P4 used are listed in Table S1. PCRs were performed in a BioRad Thermal Cycler using Takara DNA polymerase (Takara Inc.).

The deletion cassettes for *chs* genes of *A. nidulans* were constructed by fusion PCR as described (Szewczyk et al., 2006). Therefore 5′UTR and 3′UTR flanking regions of 1.5 kb size were amplified from genomic DNA of the parental strain *A. nidulans* A4, using primer pairs KO-P1/KO-P2 and KO-P3/KO-P4 listed in Table S1. These were fused to the resistance marker *ptrA*. The deletion of *chsA*, *csmB* and *chsG* in *A. nidulans* was done by polyethylene glycol mediated protoplast fusion as described before (Bayram et al., 2008).

Table 1
Strains used or generated in this study.

Strains	Genotype	Source
Neurospora crassa		
N1	*mat a*	FGSC#988
N150	*mat A*	FGSC# 9013
SMRP24	*mat A his-3⁻; Δmus-51::bar⁺*	FGSC#9717
SMRP25	*mat a; Δmus-51::bar⁺*	FGSC#9718
N39	*mat A; fl*	FGSC#4317
N40	*mat a; fl*	FGSC#4347
SMRP55	*mat A; Pccg-1::chs-1::sgfp::his-3⁺*	Sánchez-León et al. (2011)
SMRP58	*mat A; Δchs-6::hph⁺; Δmus-51*	FGSC#13408
SMRP59	*mat a; Δchs-6::hph⁺; Δmus-51*	FGSC#13409
SMRP64	*mat a; Δchs-1::hph⁺; Δmus-51*[a]	FGSC#14318
SMRP65	*mat A; Δchs-1::hph⁺; Δmus-51*[a]	FGSC#14319
SMRP66	*mat a; Δchs-3::hph⁺; Δmus-51*	FGSC#14320
SMRP67	*mat A; Δchs-3::hph⁺; Δmus-51*	FGSC#14321
SMRP81	*mat A; Pccg-1::sgfp::his-3⁺; Δmus-51*	Riquelme Lab
SMRP90	*mat A; Pccg-1::chs-1::mchfp::his-3⁺; Δmus-51*	Verdín et al. (2009)
SMRP147	*mat A; Δchs-7::hph⁺; Δmus-51*	FGSC#21365
SMRP148	*mat a; Δchs-7::hph⁺; Δmus-51*	FGSC#21364
SMRP210	*mat A; Δchs-4::hph⁺; Δmus-51*[a]	FGSC#18993
SMRP211	*mat a; Δchs-4::hph⁺; Δmus-51*[a]	FGSC#18992
SMRP212	*mat A; Δchs-5::hph⁺; Δmus-51*	FGSC#21365
SMRP213	*mat a; Δchs-5::hph⁺; Δmus-51*	FGSC#21364
SMRP282	*mat A; Δchs-2::hph⁺; Δmus-51*	FGSC#22804
NRAF3d	*mat a; Δchs-1::hph⁺; Δchs-3::hph⁺; Δmus-51*	This study
NRAF2	*mat a; Pchs-2::chs-2::gfp; Δmus-51::bar⁺*	This study
NRAF2b	*mat a; Pchs-2::chs-2::gfp; Δmus-51::bar⁺; Pccg-1::chs-1::mchfp::his-3⁺*	This study
NRAF4	*mat a; Pchs-4::chs-4::gfp; Δmus-51::bar⁺*	This study
NRAF5	*mat a; Pchs-5::chs-5::gfp; Δmus-51::bar⁺*	This study
NRAF5b	*mat a; Pchs-5::chs-5::gfp; Δmus-51::bar⁺; Pccg-1::chs-1::mchfp::his-3⁺*	This study
NRAF7	*mat a; Pchs-7::chs-7:sgfp; Δmus-51::bar⁺*	This study
Aspergillus nidulans		
AGB551	*pyroA4, pyrG89, argB2, ΔnkuA::argB*	Bayram et al. (2012)
AGB955	*pyroA4, pyrG89, argB2, ΔnkuA::argB, ΔchsA::ptrA*	This study
AGB956	*pyroA4, pyrG89, argB2, ΔnkuA::argB, ΔchsG::ptrA*	This study
AGB957	*pyroA4, pyrG89, argB2, ΔnkuA::argB, ΔcsmB::ptrA*	This study

[a] Heterokaryon strain.

Conidia of *N. crassa* strain FGSC#9718 (Δ*mus-51*, mat *A*) were transformed with DNA fragments obtained from fusion PCR (Riquelme et al., 2014), by electroporation on a BioRad Gene Pulser (25 μF capacitance, 1.5 kV voltage, and 600 ohms resistance). hygromycin (300 μg/ml) resistant heterokaryon transformants (CHS-2-GFP, CHS-4-GFP, CHS-5-GFP and CHS-7-GFP) showing fluorescence were selected (TRAF2, TRAF4, TRAF5 and TRAF7, respectively) and subsequently crossed with WT strain N150 to obtain homokaryon strains NRAF2, NRAF4, NRAF5 and NRAF7 (Table 1).

Correct integration in the selected NRAF strains was verified by PCR as described previously (Fajardo-Somera et al., 2013). Mycelium for genomic DNA extraction was grown at 28 °C for 7 days on liquid VMM without shaking or light, filtered, submerged in liquid nitrogen and lyophilized. DNA was extracted with the DNA-easy Plant extraction kit (Qiagen). PCR was performed in a T100™ Thermal cycler (BioRad) using DreamTaq DNA polymerase (Thermo Scientific) according to the manufacturer's instructions to amplify the knockout cassette and the ORF from genomic DNA of the corresponding strain. Custom designed primer pairs (Integrated DNA Technologies, Inc.) are listed in Table S1. Genomic DNA extracted from *N. crassa* strains FGSC#9718 and FGSC#988 were used as controls.

2.3. Neurospora genetic methods

Sexual crosses to generate *chs* double mutants were set up for Δ*chs-1*; Δ*chs-3*, Δ*chs-1*; Δ*chs-6*, Δ*chs-3*; Δ*chs-6*, Δ*chs-1*; Δ*chs-3*, Δ*chs-5*; Δ*chs-6*, Δ*chs-5*; Δ*chs-7*, and Δ*chs-6*; Δ*chs-7*. Perithecia and ascospores were observed for Δ*chs-1*; Δ*chs-3*, Δ*chs-5*; Δ*chs-6* and, Δ*chs-5*; Δ*chs-7*. The progeny (ascospores) was collected and activated by heat shock at 60 °C for 1 h. One hundred hygromycin resistant colonies were selected from each fertile cross. Double deletions were corroborated by PCR. Insertion of the corresponding knockout cassette was corroborated using primer pair hphSM-F/chs-P4R. Only one viable double mutant strain could be recovered for Δ*chs-1*; Δ*chs-3*. Absence of ORFs was tested with the corresponding primer pairs P1/P2 for *chs-2*, *chs-4*, *chs-5*, and *chs-7* gene (Fig. Suppl. S1) and with primer pairs pMR9–pMR10 and pMR11–pMR12 (Table S1) for *chs-3* and *chs-6* genes, respectively.

2.4. Microscopy and image processing

Cell morphology was analyzed on an inverted microscope (Zeiss Axiovert 200) coupled to a high-resolution digital camera (Zeiss Axiocam HRc). Hyphae were observed by bright field optics. A 100× (PH3) Plan Neofluar oil-immersion objective (numerical aperture [NA], 1.3) was used for image acquisition, and the images were captured with AxioVision LE software (version 4.5; Carl Zeiss).

Cells expressing GFP or mChFP tagged CHS, or stained with fluorescent dyes, were imaged using an inverted Zeiss Laser Scanning Confocal Microscope (LSM-510, Carl Zeiss, Göttingen, Germany) and an Olympus FluoView™ FV1000 inverted Confocal Microscope (Olympus, Japan), both fitted with an argon ion laser with a GFP filter set 488 nm excitation, 505–550 nm emission and He/Ne1 laser with a RFP filter set 543 nm excitation, 560 nm emission. An oil immersion objective 100× (PH3), plan neofluar (NA, 1.3) was used for LSM-510. For FV1000, an oil immersion objective 60×, (NA, 1.42) was used. Fluorescence and either phase-contrast or Differential Interference Contrast (DIC), were combined to obtain a

simultaneous view of the fluorescently labeled proteins and the entire cell. 3D-Projections in *Y* and *X* axes of septa were performed using 50 z-stacks. Septa were quantified and distances between the tip and the closest septum, and from this septum to the second septum were measured. Confocal images were captured using LSM-510 software (version 3.2; Carl Zeiss) or Olympus Fluo View software (version 4.0a), and analyzed with LSM 510 Image Examiner (version 3.2), or Olympus FV10-ASW (Version 04.00.02.09). Some of the time series were converted into animation movies using the same software.

2.5. Fluorescent dyes

Solophenyl flavine *7GFE*, a dye that binds to cell wall polysaccharides (Hoch et al., 2005), was used to stain the cell wall in living cells. A 10-fold dilution from 0.1% (w/v) stock solution in water was used as working solution. FM4-64 was used as a marker of the Spk at a final concentration of 10 μM in VMM.

2.6. Chitin content assay

Chitin content in single and double mutants was determined by the Morgan–Elson method (Morgan and Elson, 1934). VMM cultures were grown at 30 °C for 20 h, harvested by filtration, and lyophilized. Five milligrams (by triplicate for each sample) of dried mycelia were ground in a mortar and placed in 1.7 ml tubes with 1 ml of 6 N HCl, incubated at 100 °C for 20 h in a water bath, and dried in a thermoblock (100 °C, 5 h) inside an extraction hood. The dried material was resuspended in 1 ml of water and insoluble material was pelleted by centrifugation at 16,000*g* for 15 min. Supernatant was transferred to a 1.7 ml tube. A 100 μl aliquot of each sample supernatant was mixed with 100 μl of 1.5 M Na_2CO_3 in 4% (w/v) acetylacetone in 0.5 ml tubes. *N*-acetylglucosamine standards were prepared from a 10 mg/ml stock solution in water in a similar manner. For control 100 μl of H_2O were used. Reactions were incubated at 100 °C for 20 min, cooled to room temperature and transferred to 1.7 ml tubes. Seven hundred microliters of 95% ethanol were added to both, samples and standards, followed by addition of 100 μl of Elrich solution (0.175 M 4-(Dimethylamino)benzaldehyde, 12 M hydrochloric acid and 100% Ethanol). This mixture was incubated for 1 h at room temperature. Absorbance readings were taken at 520 nm using a Spectrophotometer (6505 UV/Vis Spectrophotometer, Jenway).

2.7. Co-immunoprecipitation assays

Putative proteins interacting with CHSs were recovered using GFP-TRAP® beads. *N. crassa* strains expressing CHS-1-GFP, CHS-4-GFP, CHS-5-GFP, and as control cytosolic GFP (SMRP55, NRAF4, NRAF5 and SMR81; 1×10^6 conidia/ml) were grown in liquid VMM at 30 °C and 200 rpm.

After 20 h incubation mycelia were harvested and washed with 0.96% NaCl, 1% DMSO, 100 mM PMSF. Then mycelia were ground in liquid nitrogen and crude extracts were prepared by adding 5 ml lysis buffer (33 mM phosphate buffer pH 8.2 and 0.3% Triton-100X; containing protease inhibitors (1.5 mM DTT, Roche® Protease inhibitors, 1.5 mM Benzamine, 1 mM PMSF) to 5 ml ground mycelium and vigorous vortexing. The homogenates were centrifuged twice at 4500 rpm for 29 min at 4 °C. Subsequently the supernatants were incubated with 30 μl agarose beads (GFP-Trap A gta-20; Chromotek) on a rotating platform for 2 h at 4 °C. The agarose beads were centrifuged at 2500 rpm at 4 °C for 2 min and supernatants were discarded. The beads were washed twice with lysis-buffer and repeated centrifugation at 2500 rpm at 4 °C for 2 min. Finally the beads were resuspended in 50 μl 3× loading dye and boiled at 95 °C for 10 min. 30 μl of the sample were separated on a SDS-gel, which was stained with Coomassie blue.

2.8. Liquid chromatography/tandem mass spectrometry (LC/MS/MS) protein identification

Coomassie stained proteins from the SDS-gel were cut into small pieces and an in-gel digestion with Sequencing Grade Modified Trypsin (Promega) was performed. After extraction of the peptides from the SDS-gel, they were separated by liquid chromatography with a RSLCnano Ultimate 3000 system. Mass identification of the peptides was done with an Orbitrap Velos Pro mass spectrometer. The raw LC/MS/MS data was analyzed with MaxQuant quantitative proteomics software in conjunction with Perseus software for statistical analysis of omics data (Cox and Mann, 2008). Proteins were considered as putative interaction partners for the CHSs if they met the following criteria: They were not present in the negative control (cytosolic GFP expressing SMRP55) and they were identified with at least 2 peptides and MS/MS-counts.

3. Results

3.1. N. crassa has one representative of each CHS class

Seven CHS encoding genes have been identified in the genome of *N. crassa* (Borkovich et al., 2004; Riquelme and Bartnicki-García, 2008). The chromosomal location of the seven *chs* genes in the genome was analyzed. *chs-2* and *chs-6* are located in chromosome IV. Both genes have the same transcription orientation, and their translational start points are separated by 118 kb. *chs-5* and *chs-7* are located nearby in chromosome IV. Their arrangement in the genome shows opposite transcription orientation, and their translational start points are separated by 10 kb. *chs-1* and *chs-3* are located in chromosome V, they have an opposite transcription orientation, and their translational start points are separated by 162 kb. The *chs-4* is the only *chs* located in chromosome I (Fig. Suppl. S2A). The predicted protein sequences for each CHS were also analyzed. The phylogenetic tree of CHSs generated with MEGA4 (Fig. Suppl. S2B), clearly shows that CHS-1, CHS-2 and CHS-3, which belong to Division I, are grouped in one separate cluster (bootstrap value of 100). CHS-4, CHS-5 and CHS-7 representing Division II, are grouped in another separate cluster; CHS-5 and CHS-7 both with an N-terminal myosin motor domain (MMD), (bootstrap value of 98). Furthermore, CHS-6 did not group with any of the other CHS (Fig. Suppl. S2B). The conserved QRRRW signature motif was found in all CHS sequences (Fig. 1); also a characteristic catalytic domain pfam03142, which is representative of the family of glycosyl hydrolases GH18, was shared. CHS classes I, II and III, belong to division 1 containing an additional pfam08407 domain, which is a sub-catalytic domain. CHS class I show also an unknown function domain at the amino terminus and CHS classes II and III present a pfam01644 domain. Division 2 contains CHS classes IV, V and VII that have a cytochrome b5-binding type domain. Only CHS classes V and VII present an N-terminal MMD domain and a C-terminal domain of chromatin-associated protein DEK. There are some differences in MMD between CHS classes V and VII; in CHS class V, the MMD contains three conserved ATP-binding motifs (P-loop, Switch I, and Switch II) thought to be essential for ATPase and motor activities, while CHS class VII have a shorter MMD with only one ATP-binding motif. CHS class VI is the only CHS with an N-terminal peptide signal. In all seven CHS classes, six to seven transmembrane domains are found (Fig. 1).

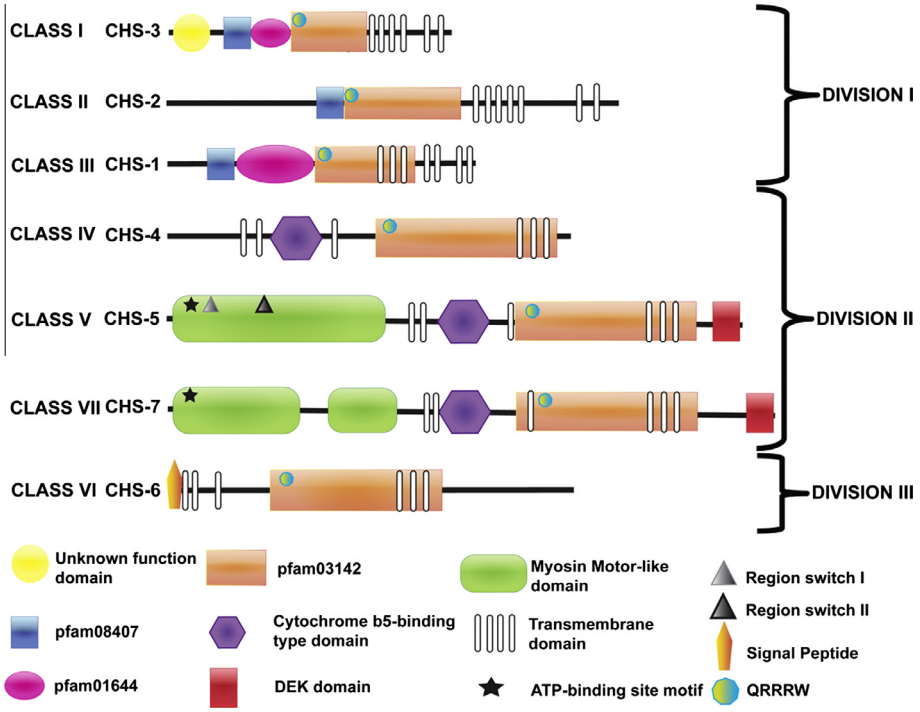

Fig. 1. Schematic representation of the seven CHS protein sequences predicted in *N. crassa*. Highlighted motifs were identified at NCBI's conserved domain database (CDD); predicted signal peptide cleavage sites were identified with Signal P (4.0), and predicted transmembrane domains were identified with TMHMM (2.0), both proteomic tools in ExPASy.

3.2. All CHSs are found at the core of the Spk and in forming septa

Previous studies have described the localization of CHS-1, -3 and -6 in *N. crassa* (Riquelme et al., 2007; Sánchez-León et al., 2011). These three CHSs were located at the core of the Spk and at forming septa. In this work we have examined the localization of the remaining CHSs in *N. crassa*. CHS-2, -4, -5, and -7 were tagged with GFP and expressed at their native loci driven by their own promoter. As for CHS-1, -3, and -6, CHS-2, -4, -5 and -7 were found at the core of the Spk (Fig. 2A–H). In addition, in subapical regions, small spots were observed (Fig. 2A, C, E and G). However, different fluorescent Spk core diameters were observed for each CHS. When co-localized with FM4-64, CHS-2-GFP seemed to occupy a smaller area at the Spk than the rest of the CHSs (Fig. 2B, D, F, and H). To discern between different CHSs, strains co-expressing CHS-1-mChFP and either CHS-5-GFP or CHS-2-GFP were analyzed. These strains were selected because CHS-5 and CHS-2 showed a different pattern of localization than the other CHSs. CHS-5-GFP occupied a larger area (diameter 1.01 ± 0.06 μm SE; $n = 10$) than CHS-2-GFP (diameter 0.89 ± 0.07 μm SE; $n = 10$ (Fig. 3A, C, D, and F). In subapical regions, small vesicles corresponding to CHS-5-GFP and CHS-1-mChFP, or CHS-2-GFP and CHS-1-mChFP did not show co-localization (Fig. 3B and E arrowheads).

During septum formation, fluorescence of GFP tagged CHS-4, -5 and -7 accumulated all around the septum similar to what was previously reported for CHS-1, -3 and -6 (Fig. 4B–D; Riquelme et al., 2007; Sánchez-León et al., 2011). After septum synthesis had been completed (a process lasting 5–10 min). CHS-2-GFP showed a distinct localization pattern at septa. CHS-2-GFP, unlike the other CHS, accumulated first at the lateral membrane during the initial steps of septum formation and progressively advanced centripetally as the septum ring expanded inwards, until localizing exclusively at the periphery of the central pore (Fig. 4A and E). CHS-4-GFP fluorescence, although found all around the septum, was especially intense at the region close to the of the pore rim (Fig. 4B arrowheads). At septa, co-localization of CHS-1 and CHS-2 was observed only at the rim of the septal pore (Fig. 4F). In 2D, CHS-1 and CHS-5 seemed to fully co-localize at septa (Fig. 4G). However, in 3D, a stronger accumulation of CHS-5-GFP around the edge of the septal pore was observed, when compared to CHS-1-mChFP, which was located along all the septum membrane (Suppl. Movie 1). In addition, we analyzed CHSs localization during conidia forming at conidiophores. CHS-4, -5 and -7 were localized in interconidial septa in both young and mature conidiophores (Fig. Suppl. S3). CHS-2-GFP went undetected during conidial formation (data not shown).

3.3. CHS-6 and CHS-7 are important for apical growth and hyphal morphology

To investigate whether all CHSs participate in vegetative growth, colony growth of *chs* deletion mutants was measured. Within the single mutants, Δ*chs-6* was the strain with the lowest growth rate, followed by Δ*chs-7* and the double mutant Δ*chs-1*; Δ*chs-3* (Table 2; Fig. 5A). In addition the Δ*chs-6* mutant also showed highly compact mycelium in comparison to the other mutants (Fig. 5A). The rest of the CHSs deletion mutants did not seem to be affected.

To examine if the Spk had been disturbed in hyphae of the mutant strains, FM4-64 was used to stain the Spk. Hyphae of Δ*chs-6*, Δ*chs-7* and Δ*chs-1*; Δ*chs-3* strains displayed the smallest Spk diameters (Table 2). The rest of *chs* deletion mutants showed a Spk diameter equivalent to that of the control strains (FGSC#988 and FGSC#9718; 1.9 ± 0.2 μm and 1.7 ± 0.1 μm SE, respectively).

3.4. CHS-3, CHS-5 and CHS-7 have an important role during asexual and sexual reproduction

Formation of aerial hyphae leads to the formation of conidiophores, the structures that give rise to conidia (asexual spores). To determine which CHSs have an important role during this

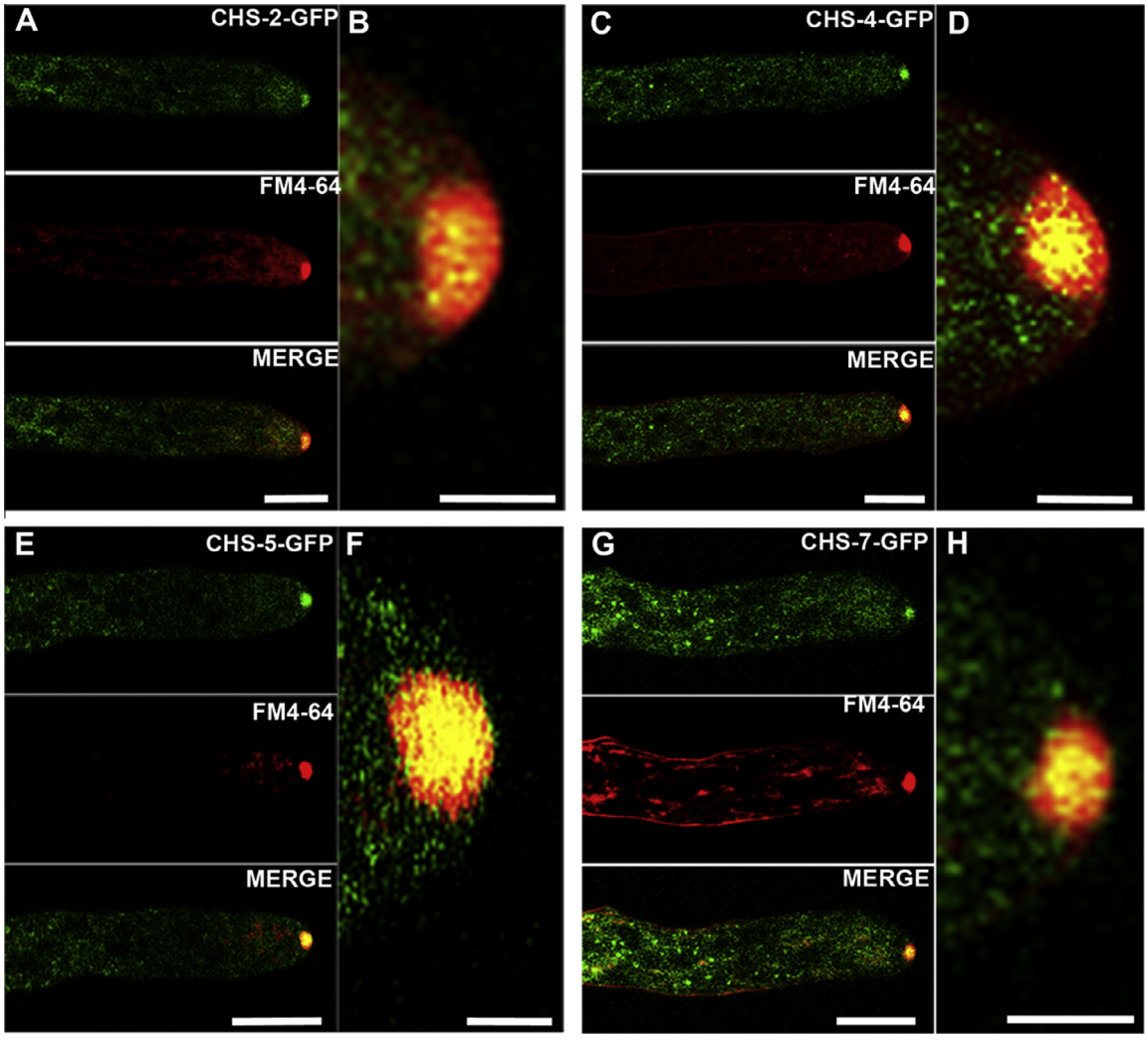

Fig. 2. CHS-2, CHS-4, CHS-5 and CHS-7 localize at the core of Spk. (A, C, E and G) At the apex CHS-2, -4, -5 and -7 tagged with GFP were localized at the core of the Spk, stained with FM4-64. Bar = 10 μm. (B, D, F and H) Magnification of the apical region in (A, C, E and G), respectively, showing co-localization (in yellow) of CHS with the core region of the FM4-64 stained Spk. Bar = 2.5 μm. (For interpretation of the references to color in this figure legend, the reader is referred to the web version of this article.)

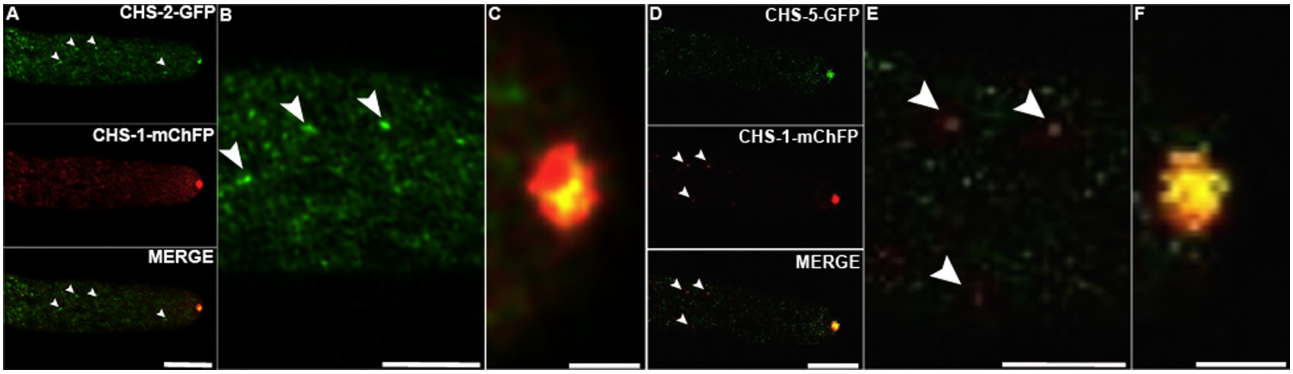

Fig. 3. CHS-1-mChFP partially colocalizes with CHS-2-GFP and CHS-5-GFP at the Spk and septa. (A) Colocalization of CHS-1-mChFP and CHS-2-GFP, and (D) CHS-1-mChFP and CHS-5-GFP at the Spk core. Bars = 10 μm. (B–C and E–F) Magnification of the subapical and apical regions of hypha in (A and D), respectively. Bars = 5 and 2.5 μm.

process, aerial hyphae formation and conidia counts were analyzed in each *chs* mutant strain. Single mutant strains Δ*chs-7*, Δ*chs-5* and double mutant strain Δ*chs-1*; Δ*chs-3* presented a reduced number of aerial hyphae (Fig. 6; Table 2). Similar results were obtained for conidia production, which were reduced in Δ*chs-5*, Δ*chs-7*, and more drastically in double mutant Δ*chs-1*; Δ*chs-3* (Table 2). Conidia and aerial hyphae production were not affected in the single mutants Δ*chs-2*, Δ*chs-3* and Δ*chs-6*.

In *N. crassa* a compatible sexual mating leads to the formation of perithecia, bottle-like structures containing the asci, which in turn

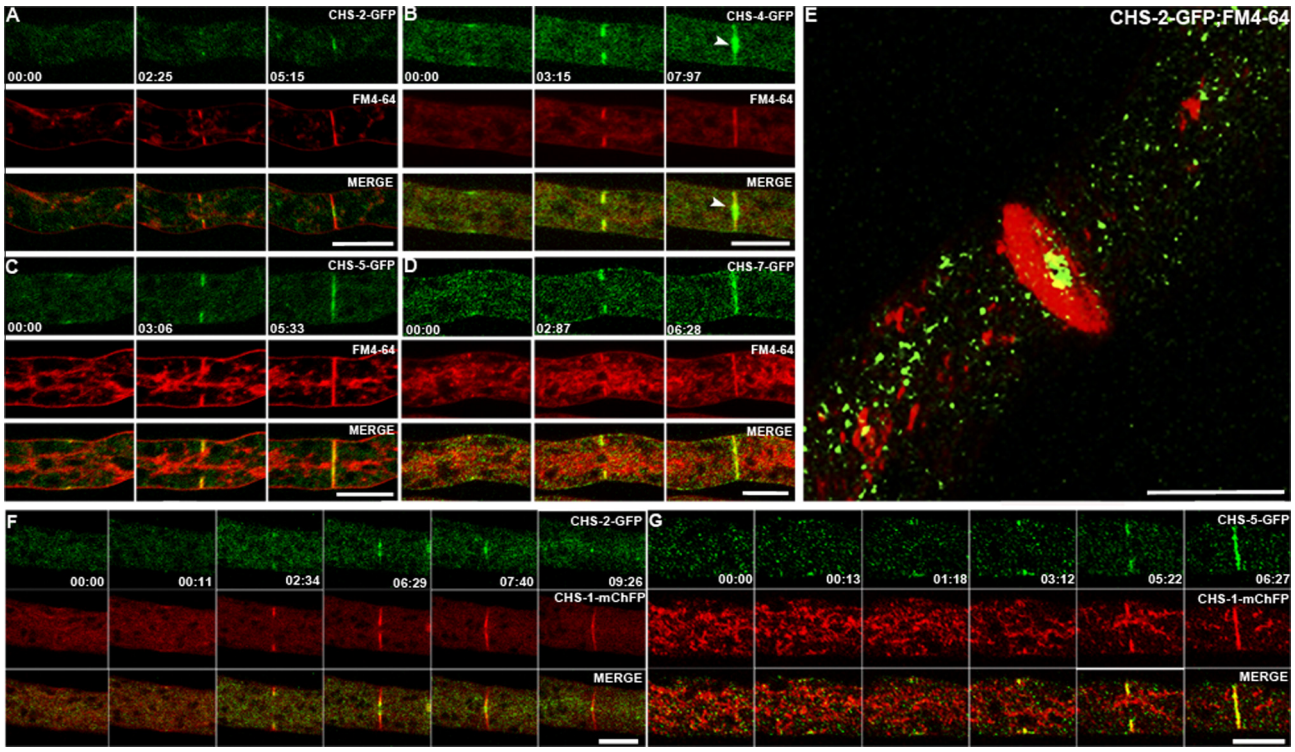

Fig. 4. CHS-2, CHS-4, CHS-5 and CHS-7 localize at developing septa. (A–D) LSCM time series showing the progressive accumulation of CHS-2, -4, -5, and -7 tagged with GFP at developing septa stained with FM4-64. Bar = 5 μm. Time in min:sec. (E) 3D projection of 100 z-stacks showing CHS-2-GFP localized around the septal pore, whereas FM4-64 stained all the septal membrane including the edge of the pore. Bar = 20 μm. (G and H) Time series showing localization of CHS-1-mChFP; CHS-2-GFP, and CHS-1-mChFP; CHS-5-GFP during septum formation. Bars = 5 μm. Time in min:sec.

Table 2
Characterization of *chsΔ* mutants.

Strains	Radial growth (cm)[a]	Growth rate (μm/min)	Hyphal diameter (μm)	Spk diameter (μm)	Aerial hyphae	Conidiation (conidia × 10^7/ml)	Perithecia formation	Ascospores released after 30 days	Chitin content (μg/5 mg)	Biomass (mg)[b]	Branching (#branches/500 μm)
FGSC#988	2.3 ± 0.3	3.36 ± 0.4	8.5 ± 0.1	1.9 ± 0.2	+++	6.4 ± 0.3	✓	––	0.59 ± 0.03	0.02 ± 0.0004	3 ± 0.19
FGSC#9718	2.8 ± 0.3	3.56 ± 0.4	10 ± 0.3	1.7 ± 0.1	+++	7.7 ± 0.04	✓	✓	0.58 ± 0.02	0.02 ± 0.0008	4 ± 0.25
Δchs-2	2.5 ± 0.3	3.5 ± 0.4	7.6 ± 1.2	1.4 ± 0.3	+++	5.6 ± 0.2	––	––	0.45 ± 0.01	0.02 ± 0.002	4 ± 0.26
Δchs-3	2.48 ± 0.02	3.42 ± 0.17	9.66 ± 0.1	1.4 ± 0.3	+++	5.7 ± 0.1	X	X	0.60 ± 0.01	0.018 ± 0.001	5 ± 0.31
Δchs-5	2.45 ± 0.03	3.66 ± 0.29	7.04 ± 0.2	1.3 ± 0.25	+	1.3 ± 0.5	✓	X	0.43 ± 0.009	**0.014** ± 0.0001	2 ± 0.18
Δchs-6	**0.63** ± 0.01	**0.87** ± 0.11	8.45 ± 0.7	1.1 ± 0.09	+++	5.1 ± 0	✓	X	**0.34** ± 0.002	**0.013** ± 0.0004	**6** ± 0.3
Δchs-7	**1.37** ± 0.01	**1.93** ± 0.5	4.44 ± 0.1	**0.9** ± 0.2	+	**0.8** ± 0.5	X	X	**0.30** ± 0.002	**0.015** ± 0.0009	2 ± 0.19
Δchs-1; Δchs-3	**1.23** ± 0.03	**1.47** ± 0.2	**4.14** ± 0.4	1.1 ± 0.2	+	**0.5** ± 0.01	––	––	**0.35** ± 0.03	**0.015** ± 0.0006	2 ± 0.19

n = 3 for growth, spk, branching, conidiation, aerial hyphae, chitin content, biomass, perithecia; ±SE 96%; X = not present; ✓ = present; +++ = normal; + = affected; –– = not done; only one mating type available for these strains; **Bold** represent the most affected.
[a] After 24 h incubation.
[b] After 48 h incubation.

contain the 8 sexual haploid ascospores. With the aim to investigate the role of each *chs* during sexual reproduction, we examined perithecia and ascospore formation in the mutant strains. Homozygotic crosses were set up for all *chs* single mutant strains. As controls, parental and WT strains were used. All crosses were performed in triplicate. After 30 days of incubation, control strains produced perithecia, and ascospores were released into the Petri dish lid (Fig. 7B and C). In contrast, Δ*chs-3 mat a* × Δ*chs-3 mat A*, and Δ*chs-7 mat a* × Δ*chs-7 mat A* crosses did not produce any perithecia (Fig. 7A). Crosses between Δ*chs-5 mat a* × Δ*chs-5 mat A*, and Δ*chs-6 mat a* × Δ*chs-6 mat A*, resulted in just a few immature perithecia, but no ascospores were released (Fig. 7A–C).

3.5. Different classes of CHS can fulfill developmental functions in fruiting body formation in different fungi

We analyzed whether these developmental functions are conserved in other fungi. We created deletion mutants for the corresponding *N. crassa chs* genes (*chs-2*, *chs-6* and *chs-7*) in *A. nidulans* (*chsA*, *chsG* and *csmB*, respectively), which were confirmed by Southern hybridization (Fig. S4). *N. crassa chs-7* is required for regular growth as well as for sexual fruiting body formation. In contrast to the *N. crassa* Δ*chs-7* mutant strains, *A. nidulans* Δ*csmB* mutants showed normal growth but presented a slight decrease in conidiospore formation (Fig. 8A). Furthermore, they were able

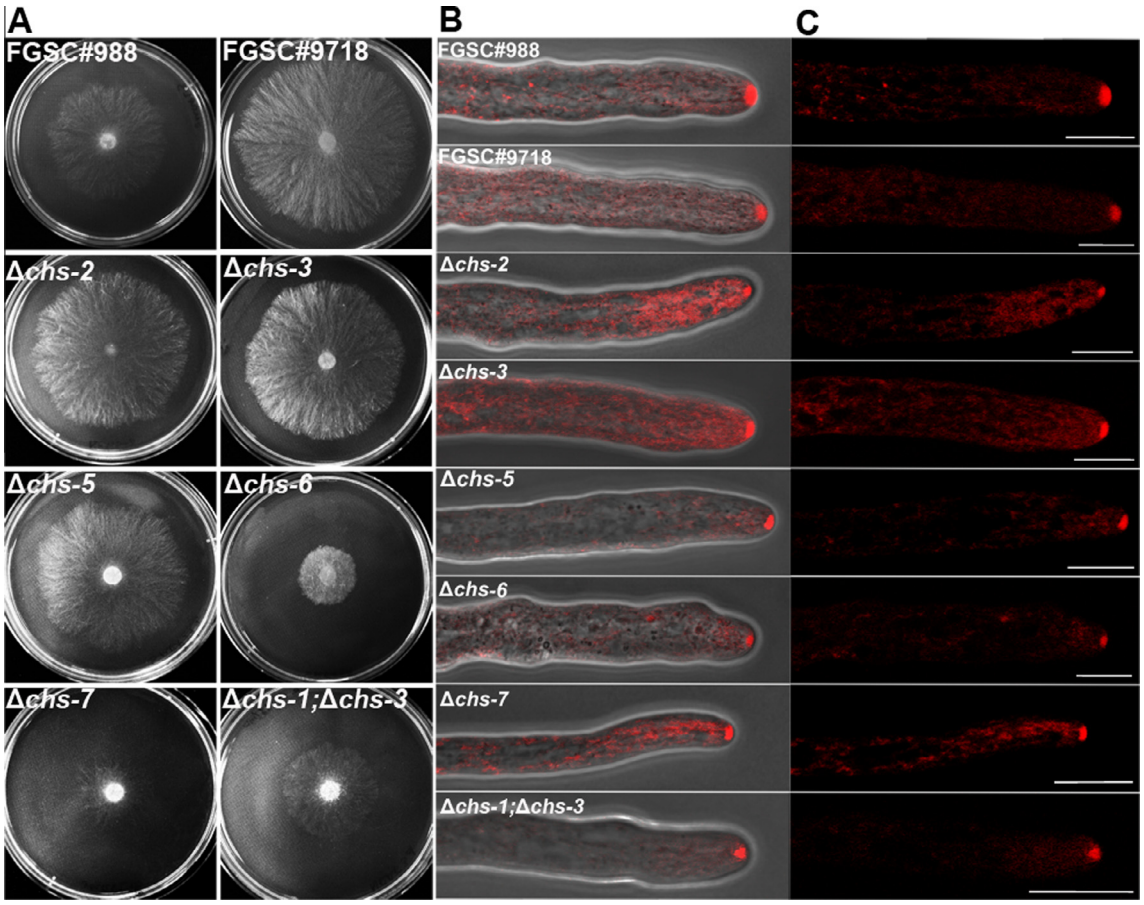

Fig. 5. Colony and hyphal morphology of *N. crassa* Δ*chs* mutant strains. (A) Colony growth of the mutant strains and two reference strains (FGSC # 988 and #9718) after 24 h of growth. (B) Overlay of phase-contrast and FM4-64. (C) Hyphal and Spk morphology of the mutant strains stained with FM4-64. Bars = 20 μm.

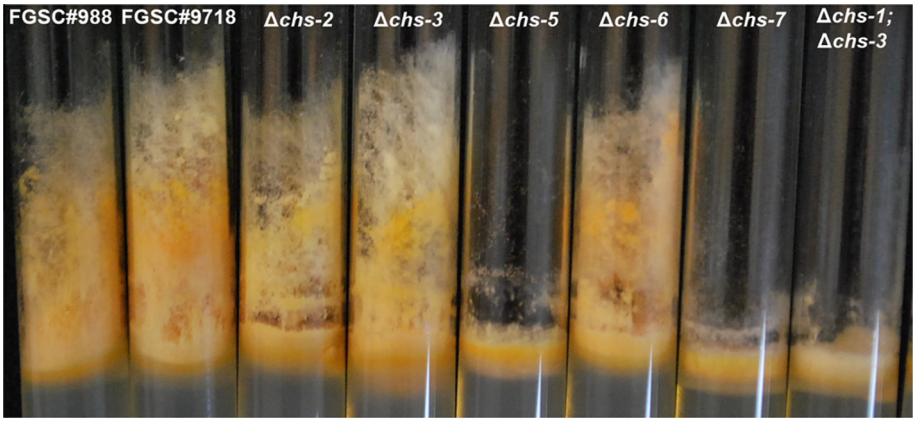

Fig. 6. Formation of aerial hyphae in *N. crassa* Δ*chs* mutant strains. *N. crassa* Δ*chs-5*, Δ*chs-7* and Δ*chs-1*; Δ*chs-3* showed a drastic reduction in aerial hyphae formation, in comparison with a *N. crassa* WT strain (FGSC#988) or the parental strain (FGSC#9718).

to complete the sexual cycle resulting in fruiting bodies (cleistothecia) with mature ascospores as the corresponding WT (Fig. 8B). *Chs-6* is involved in vegetative growth in *N. crassa.* The corresponding Δ*chs-6* mutant strain displayed slow colony growth and apical hyperbranching (Figs. 5A and 9). Deletion of the *chs-6* homologue in *A. nidulans chsG* did not result in any phenotype during colony growth or sexual development (Fig. 8A and B).

We next addressed whether another CHS is required for sexual development of *A. nidulans*. *N. crassa Δchs-2* did not exhibit any phenotype, whereas the corresponding *A. nidulans* gene *chsA*/*chs-2* had been described to be involved in asexual development (Culp et al., 2000). We deleted *chsA* and the resulting strain showed normal colony growth combined with a reduced production of conidia, which lacked the characteristic green pigment of *A. nidulans* and also displayed a red color when the plates were observed from the bottom that indicates an altered secondary metabolism for this mutant (Fig. 8A). In contrast to the *N. crassa* Δ*chs-2* strain, which displayed normal sexual fruiting bodies, the *A. nidulans* Δ*chsA* mutant was impaired in fruiting body formation, and produced only "nests" or arrested pre-cleistothecia (Fig. 8B).

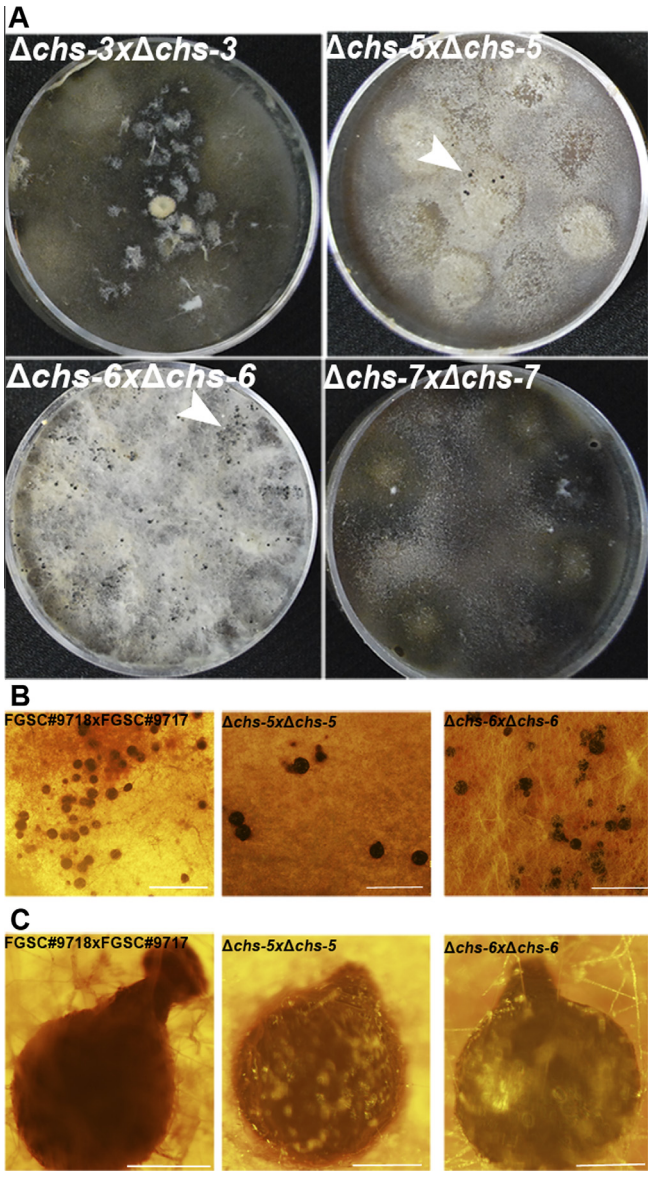

Fig. 7. Sexual development in *N. crassa* Δ*chs* mutant strains. (A) Homozygous crosses showing perithecia formation (arrowheads) only for Δ*chs-5* × Δ*chs-5* and Δ*chs-6* × Δ*chs-6*. Note the lack of perithecia for Δ*chs-3* × Δ*chs-3* and for Δ*chs-7* × Δ*chs-7*. (B) Magnification in stereoscope (10×) of perithecia resulting from fertile crosses. (C) Magnification in stereoscope (90×). Bars = 0.5 and 1 mm.

3.6. CHS-6 has an important role in branching and septation

In filamentous fungi, both branching and septum formation are cell wall expansion processes that require chitin synthesis. In order to investigate which *chs* is involved in these processes, we examined branching and septum formation in each *chs* deletion mutant. In Δ*chs-3* mutant strain a slightly higher number of branches (5 branches/500 μm; $n = 20$) was observed than in the control strains (3–4 branches; $n = 20$; Fig. 9; Table 2). In Δ*chs-6* an apical hyperbranching phenotype (6 branches/500 μm; $n = 20$) was observed (Fig. 9; Table 2). In contrast, Δ*chs-5*, Δ*chs-7* and the double mutant Δ*chs-1*; Δ*chs-3* presented fewer number of branches (2 branches/500 μm; $n = 20$) than the control strains (Fig. 9; Table 2).

None of the mutants displayed significant differences, in terms of number and position of septa in comparison to the WT control strains (FGSC#9718 and FGSC#988; Table 3; Fig. 10). However, the distance between the tip and the first septum was shorter in the Δ*chs-6* strain (220 μm; $n = 20$) than in control strains (263–278 μm; $n = 20$). Furthermore, the Δ*chs-6* strain also showed a shorter distance between the first and second septum (72 μm, $n = 20$), compared to control strains (FGSC#9718 and FGSC#988; 122–110 μm, $n = 20$ respectively).

3.7. Δchs-6 and Δchs-7 mutants displayed less chitin content

The chitin content of the cell wall was analyzed in each Δ*chs* mutant, to investigate whether the absence of a specific *chs* gene alters cell wall composition. Mutant strains Δ*chs-6*, Δ*chs-7*, and double mutant Δ*chs-1*; Δ*chs-3* presented lower *N*-acetylglucosamine concentration (0.34, 0.30, 0.35 μg/ml, respectively) than the WT control strains (0.59, 0.58 μg/ml; Table 2). Mycelium biomass (dry weight) was reduced in those strains with reduced chitin content (Δ*chs-6*, 0.013 mg; Δ*chs-7*, 0.014 mg, FGSC#988, 0.022 mg; FGSC#9718, 0.024 mg) as well as in Δ*chs-3* and Δ*chs-5* strains (0.018 mg and 0.014 mg respectively) with no apparent reduction in chitin content or growth rate, but less production of aerial hyphae and conidia (Table 2).

3.8. Putative proteins are involved in the traffic and regulation of CHS in N. crassa

Interacting proteins of CHSs were identified to obtain further insights in the distinct cellular functions of CHSs. Immunoprecipitations of GFP-tagged versions of CHS-1, CHS-4 or CHS-5 were performed and analyzed with LC/MS/MS. We considered proteins as putative interaction partners if they were at least identified with two peptides and were not present in the control strain, which expressed cytosolic GFP. We choose CHS-1 and CHS-5 because they are exclusive from filamentous fungi. Moreover, CHS-5 contains a myosin motor domain, and CHS-4 was selected because it is the homologue of Chs3p in *S. cerevisiae*, which is the most important CHS, responsible for synthesizing up to 90% of the cellular chitin (Shaw et al., 1991). A summary of the results is given in Fig. 11 and Tables S2–S4.

In total we could identify 37 putative interacting proteins for CHS-1, 21 for CHS-4 and 23 for CHS-5. Surprisingly, none of the CHSs co-precipitated with another CHS, although they share the same localization inside the hyphae. Among the identified proteins we found six shared proteins, which were present together with all three CHSs. Among these we found YPT-1, which is a small GTP-binding protein with a proposed function in protein transport. YPT-1 might be involved in the trafficking of all CHSs. Another protein with predicted vesicular transport, NCU02263 (SEC-14) was identified as interacting protein for CHS-1 as well as for CHS-4. It might also co-purify with CHS-5, where it was only partially supported because we found only one peptide, which is below our threshold for CHS-5 interacting proteins. We identified several positive candidate proteins, which are involved in cell redox homeostasis, like CAT-1 and GCY-1. Especially for CHS-1 we could identify four more proteins with oxidoreductase activity. For CHS-4 and CHS-5 we could identify the serine protease p2 (NCU00673) as a putative interacting protein. Other regulatory proteins we could identify as interaction partners for CHS-4 were a serine/threonine phosphatase PP1 (NCU00043) and a protease inhibitor (NCU06524).

4. Discussion

The genomes of filamentous fungi contain more than ten CHS encoding sequences, which are classified in seven classes, in turn grouped in three divisions (Choquer et al., 2004; Mandel et al., 2006; Pacheco-Arjona and Ramirez-Prado, 2014; Riquelme and

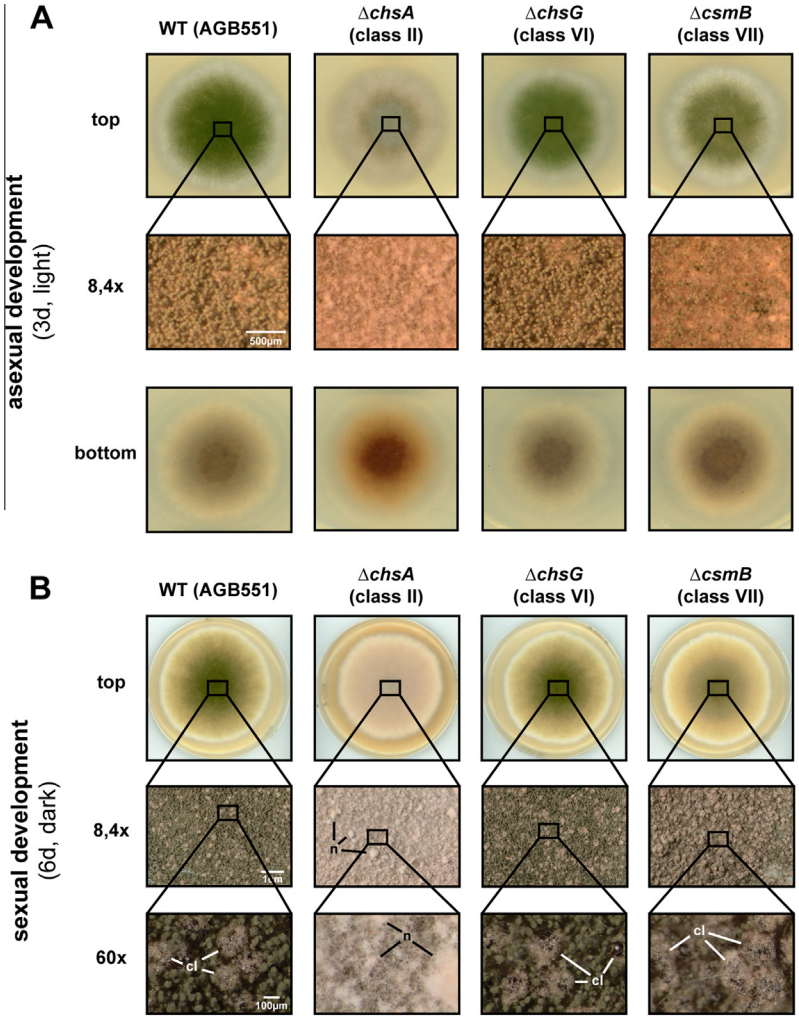

Fig. 8. Asexual and sexual development of *Aspergillus nidulans Δchs* mutants. (A) Asexual development of *A. nidulans* Δ*chsA*, Δ*csmB* and Δ*chsG*. Conidia (5×10^3) were point inoculated on a MM agarose plate and grown for 3 days at 37 °C. Top: pictures taken from above the agar plates to show colony growth and conidiation; center row: magnification of the top view at 8.4×. Bottom: pictures taken from below the agar plates to show secreted metabolites into the medium. Note the red color for Δ*chsA*, characteristic for altered secondary metabolism. (B) Sexual development of the *Aspergillus Δchs* mutant strains. Conidia (10^4) were equally plated on a MM agarose plate and incubated with limited oxygen supply in darkness. Shown are sexual fruiting bodies (cleistothecia) under binocular with magnifications of 8.4× and 60×.

Bartnicki-García, 2008; Sheng et al., 2013). *N. crassa*, as *Magnaporthe grisea*, *Fusarium oxisporum* and *Wangiella dermatitis*, has one representative for each CHS class (Kong et al., 2012; Riquelme and Bartnicki-García, 2008); while *A. nidulans* (class III; *chsB* and *chsF*), *A. fumigatus* (class III; *chsC* and *chsG*), *F. verticillioides* (class III; FvCHS3a and FvCHS3b) and *U. maydis* (class I; *Umchs3* and *Umchs4*; class IV *Umchs5* and *Umchs7*), contain eight *chs* genes (Larson et al., 2011; Mellado et al., 2003; Munro and Gow, 2001; Weber et al., 2006). In addition *B. cinerea* has seven genes for CHSs. However, it has two representatives for class III (chs3*a* and chs3*b*) and no representative for class V (Choquer et al., 2004). In different ascomycetes species, class V and VII are located nearby within the same chromosome, in opposite direction of the transcription start point (Kong et al., 2012; Mandel et al., 2006; Martin-Urdiroz et al., 2008; Takeshita et al., 2006), similar to what we found in *N. crassa* for *chs-5* and *chs-7*. However, the evolutionary history that can be inferred from the arrangement of these genes in the genome so far has not been associated with a specific CHS role or localization. It has been speculated that deletion of a CHS gene can perturb the chromatin structure of the corresponding promoter region, and influence the expression of another nearby CHS gene (Takeshita et al., 2006). Recently, a large-scale phylogenetic study of CHS in 54 fungal genomes has identified a correlation between distribution patterns of *chs* genes and fungal taxa (Pacheco-Arjona and Ramirez-Prado, 2014). This study further identified, within the genus Aspergillus, that the *chs* genes (centered on class IV) might be part of putative cell wall metabolism gene clusters (Pacheco-Arjona and Ramirez-Prado, 2014). In *N. crassa*, we found that CHS-4 (class IV) is very close on chromosome I to a putative chitin synthase activator (*csa-1*). In *S. cerevisiae*, a direct interaction between Chs3p and its activator Chs4p has been shown by two-hybrid analysis (DeMarini et al., 1997). A specific domain in Chs3p, named MIRC3-4 (Maximum Interacting Region of Chs3p with Chs4p), interacts with Chs4p. This domain was also identified in *N. crassa* CHS-4 (Park et al., 2002). Therefore it would make sense to predict that CHS-4 needs an activator for its function. To identify putative interacting partners of *N. crassa* CHSs with a potential role in their traffic and activation, we immunoprecipitated the proteins that interact with CHS-1-GFP, CHS-4-GFP, and CHS-5-GFP. Several distinct proteins putatively involved in CHS activity regulation or in biogenesis and traffic of CHS vesicular carriers to their target sites, were identified for each type of CHS, suggesting different biogenesis routes and regulatory mechanisms for the proposed different types of chitosomes. *S. cerevisiae* Chs3p besides activation,

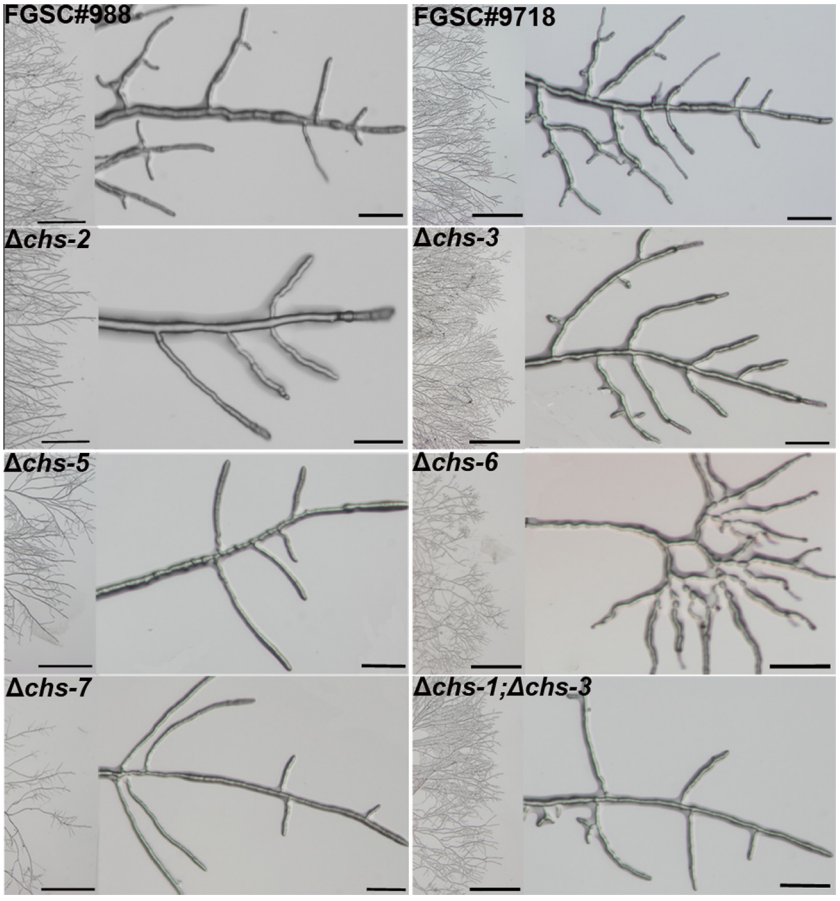

Fig. 9. Branching in *N. crassa* Δ*chs* mutant strains. Edge of colonies observed with a stereoscope (left 7× and right 90× magnification). Bars = 2 mm and 100 μm.

Table 3
Analysis of septation in *Δchs* mutant strains.

Strains	Number of septa[a]	Distance from tip to 1st septum (μm)	Distance between 1st and 2nd septum (μm)
FGSC#9718	3 ± 0.2	263	122
FGSC#988	2 ± 0.17	278	110
Δchs-2	3 ± 0.4	278	133
Δchs-3	3 ± 0.5	240	94
Δchs-5	3 ± 0.2	269	105
Δchs-6	**4 ± 0.4**	220	72
Δchs-7	3 ± 0.7	260	114
Δchs-1; Δchs-3	3 ± 0.8	250	95

Bold represents the most affected.
[a] Septa in the first 500 μm from tip. ±SE-96%.

requires the participation of different groups of auxiliary proteins that guarantee its correct spatial and temporal location (DeMarini et al., 1997; Sanchatjate and Schekman, 2006; Trautwein et al., 2006; Trilla et al., 1999; Wang et al., 2006). Transport of Chs3p to the PM requires an exomer-dependent pathway in *S. cerevisiae* (Bulawa, 1993; DeMarini et al., 1997; Grabinska et al., 2007). Prior to arrival to the PM, Chs3p interacts with the chaperone Chs7p to exit the ER and with the exomer complex (Chs5p, and the CHAPs Chs6p, Bch1p, Bch2p and Bud7p) to exit Golgi (Sanchatjate and Schekman, 2006; Santos and Snyder, 1997; Trautwein et al., 2006; Trilla et al., 1999; Ziman et al., 1998). Chs4p not only activates Chs3p but also mediates its location in the PM of the mother cell at the site of formation of the chitin ring before budding. There, it interacts with Bni4p, which in turn associates with septins (DeMarini et al., 1997; Kozubowski et al., 2003; Sanz et al., 2004). More recent studies identified the existence of an exomer-independent pathway that transports Chs3p to and from early endosomes to maintain an intracellular reservoir (Starr et al., 2012). This pathway is determined by adaptor proteins-dependent signals present at the N-terminus of Chs3p. No homologues of the proteins belonging to the yeast Chs3p exomer-dependent or independent pathways were identified in the immunoprecipitated proteins obtained for *N. crassa* CHS-1-GFP, CHS-4-GFP and CHS-5-GFP. However, this may be due to transient or weak interactions between CHS-4 and the putative interacting proteins.

CHS-2, -4, -5, and -7 had a similar subcellular localization at the Spk core during vegetative growth in *N. crassa* to the previously described localization for CHS-1, -3, and -6 (Riquelme et al., 2007; Sánchez-León et al., 2011). The localization of CHSs at the apical region indicates synthesis of new cell wall at the tip, consistent with previous reports, where monomers of *N*-acetylglucosamine, the substrate for CHSs, were found in high concentrations at the apical region (Bartnicki-García and Lippman, 1969). Studies in other fungi such as *A. nidulans* and *U. maydis* have also shown localization of CHSs at hyphal apical regions (Takeshita et al., 2005; Weber et al., 2006). All CHSs were found, both at the Spk and at developing septa. In contrast, in *U. maydis* only four of the eight CHSs (CHS5 and CHS7, class IV; CHS6 and Mcs1, class V) were located in the apical region, while the remaining CHSs were located exclusively at septation sites, in both yeast and filamentous forms (Weber et al., 2006). In *N. crassa*, each CHS occupied different regions within the Spk core. CHS-5 and CHS-1 showed partial colocalization in the Spk. CHS-2 and CHS-7 occupied a smaller area

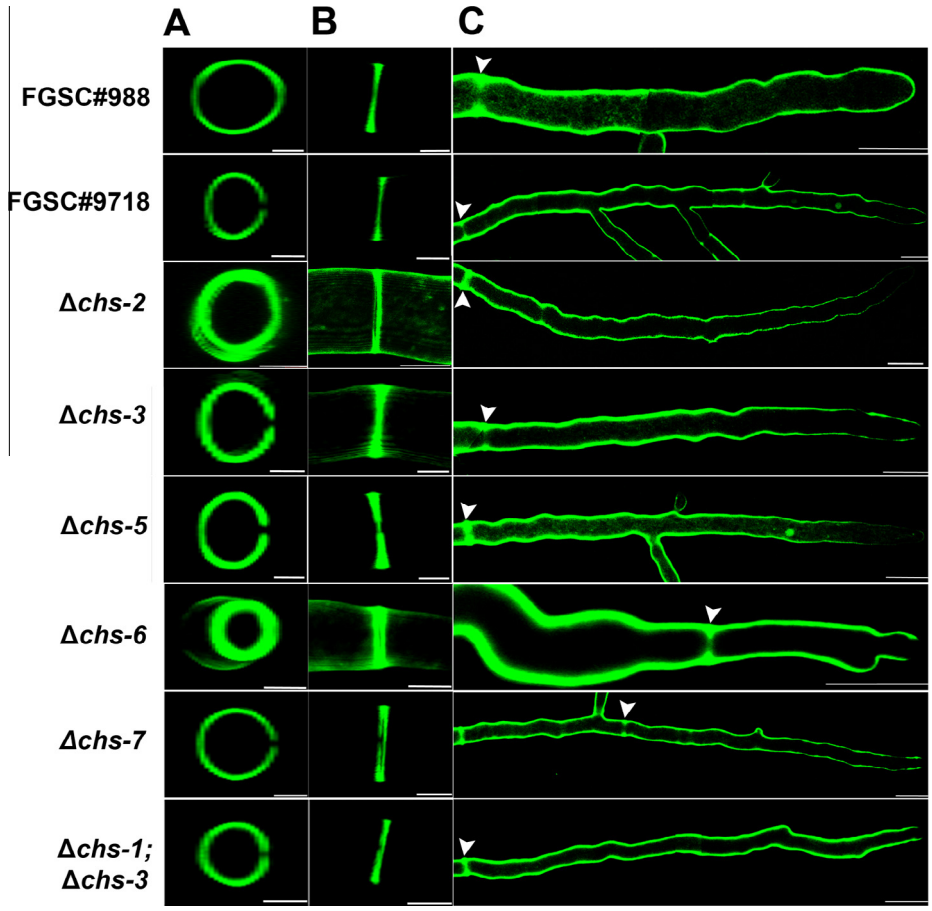

Fig. 10. Septation in *N. crassa* Δ*chs* mutant strains. (A and B) 3D projection of 50 z-stacks in longitudinal (*X*) and transversal (*Y*) views of septa stained with Solophenyl flavine 7GFE 500 in the Δ*chs* mutant strains. (C) Reconstruction in 2D of the first 500 μm of hyphae of Δ*chs* mutant strains, stained with Solophenyl flavine 7GFE 500. Bars = 5 and 10 μm. Arrowheads indicate first septum from the tip in hyphae.

than CHS-1. In previous studies a partial colocalization of CHS-3, CHS-1 and CHS-6 had been also observed in the center of the Spk (Sánchez-León et al., 2011). Similarly, the distribution of CHSs at septa varied for the different classes of CHSs. CHS-2 was the only CHS that accumulated at the edge of the septal pore, with a similar distribution than the contractile actomyosin ring, which remains associated with the advancing edge of the septum during septum development (Delgado-Alvarez et al., 2014). In *S. cerevisiae* Chs2p has an important stabilization role during the establishment of the contractile ring in cell separation (VerPlank and Li, 2005). However, *N. crassa* Δ*chs2* was not impeded in septum formation. Moreover, CHS-4 was distributed all around the septum accumulated more intensely around the septal pore, and the remaining CHSs showed a normal distribution around septum. These differences provide additional proof that the different CHSs are transported in different populations of chitosomes, as previously described for CHSs classes I, III and VI (Fig. 12A) (Riquelme et al., 2007; Sánchez-León et al., 2011).

One of the interacting proteins identified for all three CHSs was the Rab GTPase YPT-1, a molecular switch that regulates different steps of the secretory pathway, including traffic of vesicles (Du and Novick, 2001; Jedd et al., 1997; Sacher et al., 2001; Suvorova et al., 2002). Recent studies in *N. crassa* have shown YPT-1 at the core of Spk, co-localizing with the CHS containing microvesicles (Sánchez-León et al., 2014), which suggests a role for YPT-1 as a regulator of chitosomes that reach the Spk. For CHS-1 and CHS-4, SEC-14, a homolog of Sec14p, a phosphatidyl inositol transfer protein essential for vesicle budding from the Golgi and for regulation of endosome trafficking in *S. cerevisiae* (Curwin et al., 2009; Sha et al., 1998), was identified. Previous studies in *N. crassa* showing brefeldin A-independent arrival of CHS-1, CHS-3 and CHS-6 to the Spk core suggested a non-conventional secretory route for CHSs (Riquelme et al., 2007; Sánchez-León et al., 2011). Additional studies are needed to further characterize the role of SEC-14 in the vesicular transport of CHS-1 and CHS-4 and to analyze whether it participates in exocytic or endosomal traffic of these CHSs. In *C. albicans* Chs3p needs to be phosphorylated for its proper localization and function, although no kinase responsible for such regulation has yet been identified (Lenardon et al., 2010). Similarly, the phosphorylated state of Chs2p in *S. cerevisiae* affects its temporal and spatial localization (Chin et al., 2012; Teh et al., 2009; VerPlank and Li, 2005; Zhang et al., 2006). Cyclin-dependent kinase Cdk1p can directly phosphorylate Chs2p. Phosphorylated Chs2p is retained in the ER until the cell comes out of mitosis (Teh et al., 2009; VerPlank and Li, 2005; Zhang et al., 2006), when Chs2p is subsequently dephosphorylated by phosphatase Cdc14p (Chin et al., 2012). In *N. crassa*, the phosphatase PP1 (NCU00043), with a potential role in dephosphorylation of CHS-4 and another protein of potentially great interest, the serine protease p2, were identified in co-immunoprecipitations of CHS-4 and CHS-5. It was previously described that CHSs are zymogen proteins, which need to be activated proteolytically (Cabib and Farkas, 1971; Duran and Cabib, 1978; Leal-Morales et al., 1988; McMurrough and Bartnicki-García, 1971; Ruiz-Herrera et al., 1975). Previous studies in *N. crassa* have shown that the total activity of CHSs requires trypsin as proteolytic activator (Arroyo-Begovich and Ruiz-Herrera,

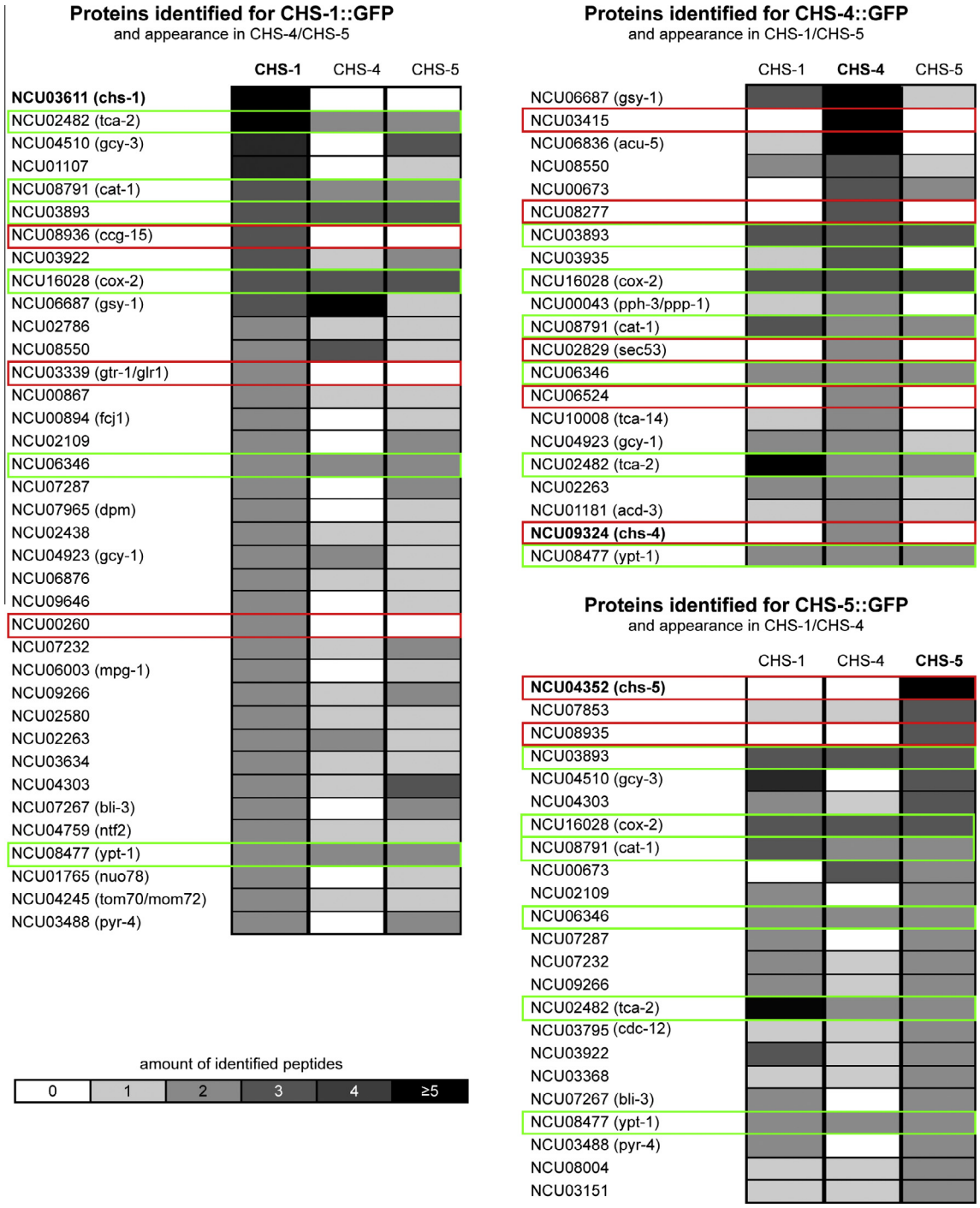

Fig. 11. Putative interacting proteins for CHS-1, CHS-4 and CHS-5 identified via LC–MS/MS. Given are the identified proteins for one particular CHS and the appearance of the proteins in identifications for the other two CHSs. Proteins which were present for all CHSs are marked in green while unique proteins for a particular CHS are marked in red. Additional information about all identified proteins is given in Tables S2–S4. (For interpretation of the references to color in this figure legend, the reader is referred to the web version of this article.)

1979). Our results suggest that the serine-type endopeptidase activity of the serine protease p2 could be involved in the activation of at least two classes of CHSs, class IV and V. The protease inhibitor identified in co-immunoprecipitations of CHS-4, could have a role inhibiting serine protease p2 during traffic of CHS-4 and until reaching its final destination at the cell sites to start making chitin. However, it is necessary to investigate whether these proteins are really able to activate and regulate the activity of a given CHS, such as CHS-4. Other proteins identified as positive candidates, participate during cell redox homeostasis, such as CAT-1 and GCY-1. These results suggest a crosstalk between a highly balanced intracellular redox level, which has important functions in cellular polarity as well as sexual development, and CHSs (Scott and Eaton, 2008).

The characterization of the Δ*chs* mutant strains revealed specific functions for CHS classes I, II, VI, V, and VII in *N. crassa* during different developmental stages. *N. crassa* Δ*chs-2* (class II) showed no affected phenotype during any of the developmental stages studied, as previously reported for a *N. crassa chs-2*^{RIP} mutant (Din and Yarden, 1994). Similar results were found for *U. maydis*,

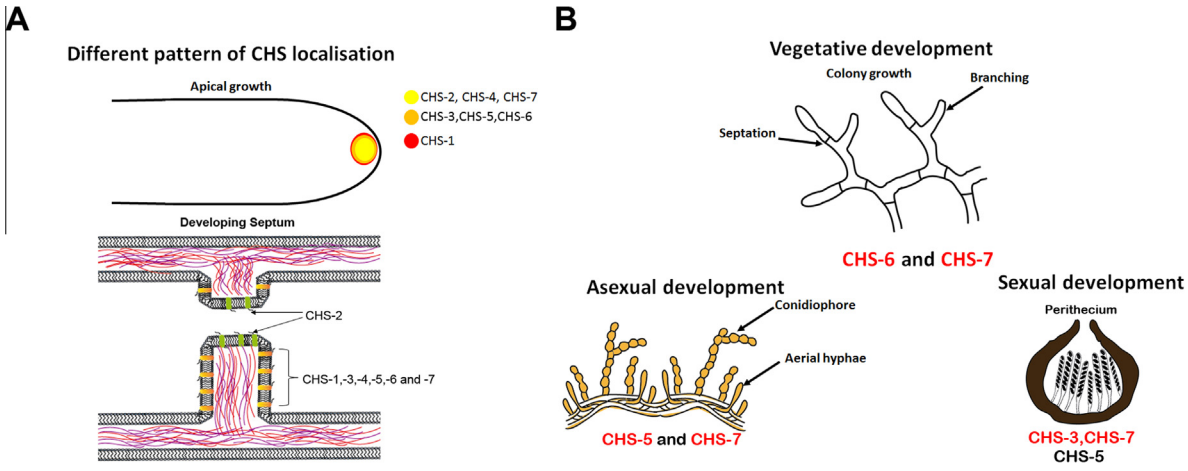

Fig. 12. Proposed model for CHSs role during developmental stages in *N. crassa*. (A) CHSs localization showed different patterns during apical growth and developing septa. Previous work on CHSs in *N. crassa* showed a partial colocalization of CHS-3, CHS-6 and CHS-1 in the Spk. In this model we show how the rest of the chitin synthases partially colocalize in the Spk and also during the formation of the septum. (B) Overview of the participation during vegetative growth, sexual and asexual development. CHS-6 and CHS-7 showed a major participation during vegetative growth. During sexual and asexual development CHS-7 also showed to be involved during these stages besides of CHS-5 (asexual development) and CHS-3 (sexual development).

where Δ*chs2* did not present any disrupted phenotype and was not affected in growth or plant infection (Weber et al., 2006). In yeast however, CHS class II has an important role. Chs2p is involved in the synthesis of the primary septum during late mitosis, a prerequisite for the separation of the daughter from the mother (Shaw et al., 1991). On the other hand, *N. crassa* Δ*chs-3* (class I) did not show any abnormalities during vegetative growth, as previously described (Sánchez-León et al., 2011). However, during sexual development, no formation of perithecia was observed 30 days post-inoculation, suggesting that CHS class I is involved in the development of sexual structures. *A. nidulans* and *A. fumigatus* class I mutants Δ*chsC* and Δ*chsA* respectively, displayed a normal phenotype compared to the WT strains (Motoyama et al., 1994; Munro and Gow, 2001). However, in other fungal species, class I CHSs seem to have an important role. For example, in *B. cinerea* chs1 is involved in hyphal growth and pathogenicity (Soulie et al., 2006; Wang et al., 2001). *N. crassa chs-1*^{RIP} (class III) mutant showed an abnormal phenotype with abnormal swelling hyphae and slow growth (Yarden and Yanofsky, 1991). In contrast, *N. crassa* Δ*chs-1* mutant (FGSC#14318) exhibited no apparent phenotype (Sánchez-León et al., 2011). In this study we have confirmed that the *N. crassa* Δ*chs-1* mutant previously analyzed did indeed contain a copy of the *chs-1* gene, in addition to the deletion cassette, indicating that the strain was in a heterokaryon condition. Therefore, it remains to be verified whether *chs-1* might have a primary role during vegetative growth of hyphae as suggested by the analysis of the *chs-1*^{RIP} mutant (Yarden and Yanofsky, 1991). *N. crassa* Δ*chs-6* mutant showed a slower growth rate than the rest of the mutants and apical hyper branching, indicating it plays a major role in apical growth. It has been previously described that apical branching is accompanied by a drastic reduction in the elongation rate of the hyphae (Riquelme and Bartnicki-García, 2004). This would explain the reduction of growth rate in the mutant Δ*chs-6*. There are very few reports about CHS class VI. In *M. grisea* it has been reported that *chs-7* (class VI) has a role in the formation of specialized infection structures (appressoria), suggesting their involvement in the invasion of host (Kong et al., 2012). CHS classes V and VII, which contain an amino terminal MMD, appear to be important in several fungal species. They are essential for apical growth and morphogenesis in *A. nidulans* (CsmA and CsmB), *C. graminicola* (ChsVb), *F. verticilliodes* (CHS5 and CHS7), *A. fumigatus* (ChsE) and *U. maydis* (Msc1) (Amnuaykanjanasin and Epstein, 2003, 2006; Larson et al., 2011; Mellado et al., 2003; Weber et al., 2006). In *N. crassa* Δ*chs-5* and Δ*chs-7* mutants showed a reduction in aerial hyphae formation, a decrease in conidia production, reduced chitin content, reduced biomass and less branches. Our results indicated also an important role for *chs-7* during formation of sexual structures (Fig. 12B). Considering the results obtained for *N. crassa* and for other filamentous fungi, it could be concluded that CHSs belonging to the same class, while having a high degree of homology, may not necessarily have a conserved function in different fungal species.

Acknowledgments

This work was supported by Mexican National Council for Science and Technology (CONACYT) grants B0C022 and CONACYT-DFG 75306 to MRP. We acknowledge CONACYT fellowship (176643) to RAFS, which allowed completion of this study. GHB and BJ were funded by the DFG German/Mexican research group FOR1334 (BR 1502/13-2).

Appendix A. Supplementary material

Supplementary data associated with this article can be found, in the online version, at http://dx.doi.org/10.1016/j.fgb.2015.01.002.

References

Amnuaykanjanasin, A., Epstein, L., 2003. A class V chitin synthase gene, chsA is essential for conidial and hyphal wall strength in the fungus *Colletotrichum graminicola* (*Glomerella graminicola*). Fungal Genet. Biol. 38, 272–285.

Amnuaykanjanasin, A., Epstein, L., 2006. A class Vb chitin synthase in *Colletotrichum graminicola* is localized in the growing tips of multiple cell types, in nascent septa, and during septum conversion to an end wall after hyphal breakage. Protoplasma 227, 155–164.

Arbelet, D., Malfatti, P., Simond-Cote, E., Fontaine, T., Desquilbet, L., Expert, D., Kunz, C., Soulie, M.C., 2010. Disruption of the Bcchs3a chitin synthase gene in *Botrytis cinerea* is responsible for altered adhesion and overstimulation of host plant immunity. Mol. Plant–Microbe Interact. J. 23, 1324–1334.

Arroyo-Begovich, A., Ruiz-Herrera, J., 1979. Proteolytic activation and inactivation of chitin synthase from *Neurospora crassa*. J. Gen. Microbiol. 113, 339–345.

Bartnicki-García, S., Lippman, E., 1969. Fungal morphogenesis: cell wall construction in *Mucor rouxii*. Science 165, 302–304.

Bartnicki-García, S., Nickerson, W.J., 1962. Isolation, composition, and structure of cell walls of filamentous and yeast-like forms of *Mucor rouxii*. Biochim. Biophys. Acta 58, 102–119.

Bartnicki-García, S., Reyes, E., 1968. Chemical composition of sporangiophore walls of *Mucor rouxii*. Biochim. Biophys. Acta 165, 32–42.

Bayram, O., Krappmann, S., Ni, M., Bok, J.W., Helmstaedt, K., Valerius, O., Braus-Stromeyer, S., Kwon, N.J., Keller, N.P., Yu, J.H., et al., 2008. VelB/VeA/LaeA

complex coordinates light signal with fungal development and secondary metabolism. Science 320, 1504–1506.
Bayram, O., Bayram, O.S., Ahmed, Y.L., Maruyama, J., Valerius, O., Rizzoli, S.O., Ficner, R., Irniger, S., Braus, G.H., 2012. The *Aspergillus nidulans* MAPK module AnSte11-Ste50-Ste7-Fus3 controls development and secondary metabolism. PLoS Genet. 8, e1002816.
Bennett, J.W., Lasure, L.L., 1991. More Gene Manipulations in Fungi. Academic Press.
Borkovich, K.A., Alex, L.A., Yarden, O., Freitag, M., Turner, G.E., Read, N.D., Seiler, S., Bell-Pedersen, D., Paietta, J., Plesofsky, N., et al., 2004. Lessons from the genome sequence of *Neurospora crassa*: tracing the path from genomic blueprint to multicellular organism. Microbiol. Mol. Biol. Rev. 68, 1–108.
Braun, P.C., Calderone, R.A., 1978. Chitin synthesis in *Candida albicans*: comparison of yeast and hyphal forms. J. Bacteriol. 133, 1472–1477.
Bulawa, C.E., 1992. Csd2, Csd3, and Csd4, genes required for chitin synthesis in *Saccharomyces cerevisiae* the Csd2 gene product is related to chitin synthases and to developmentally regulated proteins in *Rhizobium* species and *Xenopus laevis*. Mol. Cell. Biol. 12, 1764–1776.
Bulawa, C.E., 1993. Genetics and molecular biology of chitin synthesis in fungi. Ann. Rev. Microbiol. 47, 505–534.
Bulawa, C.E., Slater, M., Cabib, E., Auyoung, J., Sburlati, A., Adair, W.L., Robbins, P.W., 1986. The *Saccharomyces cerevisiae* structural gene for chitin synthase is not required for chitin synthesis *in vivo*. Cell 46, 213–225.
Bulawa, C.E., Miller, D.W., Henry, L.K., Becker, J.M., 1995. Attenuated virulence of chitin-deficient mutants of *Candida albicans*. Proc. Natl. Acad. Sci. USA 92, 10570–10574.
Cabib, E., Farkas, V., 1971. The control of morphogenesis: an enzymatic mechanism for the initiation of septum formation in yeast. Proc. Natl. Acad. Sci. USA 68, 2052–2056.
Cassone, A., 1986. Cell wall of pathogenic yeasts and implications for antimycotic therapy. Drugs Exp. Clin. Res. 12, 635–643.
Chin, C.F., Bennett, A.M., Ma, W.K., Hall, M.C., Yeong, F.M., 2012. Dependence of Chs2 ER export on dephosphorylation by cytoplasmic Cdc14 ensures that septum formation follows mitosis. Mol. Biol. Cell 23, 45–58.
Choquer, M., Boccara, M., Goncalves, I.R., Soulie, M.C., Vidal-Cros, A., 2004. Survey of the *Botrytis cinerea* chitin synthase multigenic family through the analysis of six euascomycetes genomes. Eur. J. Biochem. 271, 2153–2164.
Cid, V.J., Duran, A., del Rey, F., Snyder, M.P., Nombela, C., Sanchez, M., 1995. Molecular basis of cell integrity and morphogenesis in *Saccharomyces cerevisiae*. Microbiol. Rev. 59, 345–386.
Cox, J., Mann, M., 2008. MaxQuant enables high peptide identification rates, individualized p.p.b.-range mass accuracies and proteome-wide protein quantification. Nat. Biotechnol. 26, 1367–1372.
Culp, D.W., Dodge, C.L., Miao, Y., Li, L., Sag-Ozkal, D., Borgia, P.T., 2000. The chsA gene from *Aspergillus nidulans* is necessary for maximal conidiation. FEMS Microbiol. Lett. 182, 349–353.
Curwin, A.J., Fairn, G.D., McMaster, C.R., 2009. Phospholipid transfer protein Sec14 is required for trafficking from endosomes and regulates distinct trans-Golgi export pathways. J. Biol. Chem. 284, 7364–7375.
Delgado-Alvarez, D.L., Bartnicki-Garcia, S., Seiler, S., Mouriño-Pérez, R.R., 2014. Septum development in *Neurospora crassa*: the septal actomyosin tangle. PLoS ONE 9, e96744.
DeMarini, D.J., Adams, A.E., Fares, H., De Virgilio, C., Valle, G., Chuang, J.S., Pringle, J.R., 1997. A septin-based hierarchy of proteins required for localized deposition of chitin in the *Saccharomyces cerevisiae* cell wall. J. Cell Biol. 139, 75–93.
Din, A.B., Yarden, O., 1994. The *Neurospora crassa chs-2* gene encodes a non-essential chitin synthase. Microbiology 140 (Pt 9), 2189–2197.
Din, A.B., Specht, C.A., Robbins, P.W., Yarden, O., 1996. Chs-4, a class IV chitin synthase gene from *Neurospora crassa*. Mol. Genet. Genom. 250, 214–222.
Du, L.L., Novick, P., 2001. Yeast rab GTPase-activating protein Gyp1p localizes to the Golgi apparatus and is a negative regulator of Ypt1p. Mol. Biol. Cell 12, 1215–1226.
Duran, A., Cabib, E., 1978. Solubilization and partial purification of yeast chitin synthetase. Confirmation of the zymogenic nature of the enzyme. J. Biol. Chem. 253, 4419–4425.
Fajardo-Somera, R.A., Bowman, B., Riquelme, M., 2013. The plasma membrane proton pump PMA-1 is incorporated into distal parts of the hyphae independently of the Spitzenkorper in *Neurospora crassa*. Eukaryot. Cell 12, 1097–1105.
Fukuda, K., Yamada, K., Deoka, K., Yamashita, S., Ohta, A., Horiuchi, H., 2009. Class III chitin synthase ChsB of *Aspergillus nidulans* localizes at the sites of polarized cell wall synthesis and is required for conidial development. Eukaryot. Cell 8, 945–956.
Glaser, L., Brown, D.H., 1957. The synthesis of chitin in cell-free extracts of *Neurospora crassa*. J. Biol. Chem. 228, 729–742.
Gooday, G.W., 1994. Physiology of microbial degradation of chitin and chitosan. In: Ratledge, C. (Ed.), Biochemistry of Microbial Degradation. Springer, Dordrecht, pp. 279–312.
Gow, N.A., Robbins, P.W., Lester, J.W., Brown, A.J., Fonzi, W.A., Chapman, T., Kinsman, O.S., 1994. A hyphal-specific chitin synthase gene (CHS2) is not essential for growth, dimorphism, or virulence of *Candida albicans*. Proc. Natl. Acad. Sci. USA 91, 6216–6220.
Grabinska, K.A., Magnelli, P., Robbins, P.W., 2007. Prenylation of *Saccharomyces cerevisiae* Chs4p affects chitin synthase III activity and chitin chain length. Eukaryot. Cell 6, 328–336.
Hearn, V.M., Sietsma, J.H., 1994. Chemical and immunological analysis of the *Aspergillus fumigatus* cell wall. Microbiology 140 (Pt 4), 789–795.
Hickey, P.C., Swift, S.R., Roca, M.G., Read, N.D., 2004. Live-cell imaging of filamentous fungi using vital fluorescent dyes and confocal microscopy. Methods Microbiol. 34, 63–87.
Hoch, H.C., Galvani, C.D., Szarowski, D.H., Turner, J.N., 2005. Two new fluorescent dyes applicable for visualization of fungal cell walls. Mycologia 97, 580–588.
Jedd, G., Mulholland, J., Segev, N., 1997. Two new Ypt GTPases are required for exit from the yeast trans-Golgi compartment. J. Cell Biol. 137, 563–580.
Kong, L.A., Yang, J., Li, G.T., Qi, L.L., Zhang, Y.J., Wang, C.F., Zhao, W.S., Xu, J.R., Peng, Y.L., 2012. Different chitin synthase genes are required for various developmental and plant infection processes in the rice blast fungus *Magnaporthe oryzae*. PLoS Pathog. 8, e1002526.
Kozubowski, L., Panek, H., Rosenthal, A., Bloecher, A., DeMarini, D.J., Tatchell, K., 2003. A Bni4-Glc7 phosphatase complex that recruits chitin synthase to the site of bud emergence. Mol. Biol. Cell 14, 26–39.
Larson, T.M., Kendra, D.F., Busman, M., Brown, D.W., 2011. *Fusarium verticillioides* chitin synthases CHS5 and CHS7 are required for normal growth and pathogenicity. Curr. Genet. 57, 177–189.
Leal-Morales, C.A., Bracker, C.E., Bartnicki-García, S., 1988. Localization of chitin synthetase in cell-free homogenates of *Saccharomyces cerevisiae*: chitosomes and plasma membrane. Proc. Natl. Acad. Sci. USA 85, 8516–8520.
Lenardon, M.D., Milne, S.A., Mora-Montes, H.M., Kaffarnik, F.A., Peck, S.C., Brown, A.J., Munro, C.A., Gow, N.A., 2010. Phosphorylation regulates polarisation of chitin synthesis in *Candida albicans*. J. Cell Sci. 123, 2199–2206.
Mandel, M.A., Galgiani, J.N., Kroken, S., Orbach, M.J., 2006. *Coccidioides posadasii* contains single chitin synthase genes corresponding to classes I to VII. Fungal Genet. Biol. 43, 775–788.
Martin-Urdiroz, M., Roncero, M.I., Gonzalez-Reyes, J.A., Ruiz-Roldan, C., 2008. ChsVb, a class VII chitin synthase involved in septation, is critical for pathogenicity in *Fusarium oxysporum*. Eukaryot. Cell 7, 112–121.
McMurrough, I., Bartnicki-García, S., 1971. Properties of a particulate chitin synthetase from *Mucor rouxii*. J. Biol. Chem. 246, 4008–4016.
Mellado, E.A.-B.A., Gow, N.A.R., Holden, D.W., 1996. The *Aspergillus fumigatus* chsC and chsG genes encode class III chitin synthases with different function. Mol. Microbiol. 20, 667–679.
Mellado, E., Dubreucq, G., Mol, P., Sarfati, J., Paris, S., Diaquin, M., Holden, D.W., Rodriguez-Tudela, J.L., Latge, J.P., 2003. Cell wall biogenesis in a double chitin synthase mutant (chsG-/chsE-) of *Aspergillus fumigatus*. Fungal Genet. Biol. 38, 98–109.
Mio, T., Yabe, T., Sudoh, M., Satoh, Y., Nakajima, T., Arisawa, M., Yamada-Okabe, H., 1996. Role of three chitin synthase genes in the growth of *Candida albicans*. J. Bacteriol. 178, 2416–2419.
Morgan, W.T., Elson, L.A., 1934. A colorimetric method for the determination of N-acetylglucosamine and N-acetylchrondrosamine. Biochem. J. 28, 988–995.
Motoyama, T., Kojima, N., Horiuchi, H., Ohta, A., Takagi, M., 1994. Isolation of a chitin synthase gene (chsC) of *Aspergillus nidulans*. Biosci. Biotechnol. Biochem. 58, 2254–2257.
Motoyama, T., Fujiwara, M., Kojima, N., Horiuchi, H., Ohta, A., Takagi, M., 1996. The *Aspergillus nidulans* genes chsA and chsD encode chitin synthases which have redundant functions in conidia formation. Mol. Genet. Genom. 251, 442–450.
Motoyama, T., Fujiwara, M., Kojima, N., Horiuchi, H., Ohta, A., Takagi, M., 1997. The *Aspergillus nidulans* genes chsA and chsD encode chitin synthases which have redundant functions in conidia formation [corrected and republished article originally appeared in Mol Gen Genet 1996 Jun, 251(4), pp. 442–50]. Mol. Gen. Genet.: MGG 253, 520–528.
Munro, C.A., Gow, N.A.R., 2001. Chitin synthesis in human pathogenic fungi. Med. Mycol. 39, 41–53.
Munro, C.A., Winter, K., Buchan, A., Henry, K., Becker, J.M., Brown, A.J.P., Bulawa, C.E., Gow, N.A.R., 2001. Chs1 of *Candida albicans* is an essential chitin synthase required for synthesis of the septum and for cell integrity. Mol. Microbiol. 39, 1414–1426.
Munro, C.A., Whitton, R.K., Bleddyn Hughes, H., Rella, M., Selvaggini, S., Gow, N.A.R., 2003. CHS8—a fourth chitin synthase gene of *Candida albicans* contributes to in vitro chitin synthase activity, but is dispensable for growth. Fungal Genet. Biol. 40, 146–158.
Pacheco-Arjona, J.R., Ramirez-Prado, J.H., 2014. Large-scale phylogenetic classification of fungal chitin synthases and identification of a putative cell-wall metabolism gene cluster in *Aspergillus* genomes. PLoS ONE 9, e104920.
Park, Y.S., Choi, S.J., Park, N.H., Kim, C.H., Kim, S.U., Choi, W., 2002. Identification of a domain in yeast chitin synthase 3 interacting with chitin synthase 4 by two-hybrid analysis. J. Microbiol. Biotechnol. 12, 943–949.
Riquelme, M., Bartnicki-García, S., 2004. Key differences between lateral and apical branching in hyphae of *Neurospora crassa*. Fungal Genet. Biol. 41, 842–851.
Riquelme, M., Bartnicki-García, S., 2008. Advances in understanding hyphal morphogenesis: ontogeny, phylogeny and cellular localization of chitin synthases. Fung. Biol. Rev. 22, 56–70.
Riquelme, M., Bartnicki-García, S., Gonzalez-Prieto, J.M., Sánchez-León, E., Verdín-Ramos, J.A., Beltran-Aguilar, A., Freitag, M., 2007. Spitzenkörper localization and intracellular traffic of green fluorescent protein-labeled CHS-3 and CHS-6 chitin synthases in living hyphae of *Neurospora crassa*. Eukaryot. Cell 6, 1853–1864.
Riquelme, M., Bredeweg, E.L., Callejas-Negrete, O., Roberson, R.W., Ludwig, S., Beltran-Aguilar, A., Seiler, S., Novick, P., Freitag, M., 2014. The *Neurospora crassa* exocyst complex tethers Spitzenkorper vesicles to the apical plasma membrane during polarized growth. Mol. Biol. Cell 25, 1312–1326.
Rogg, L.E., Fortwendel, J.R., Juvvadi, P.R., Lilley, A., Steinbach, W.J., 2011. The chitin synthase genes chsA and chsC are not required for cell wall stress responses in

the human pathogen *Aspergillus fumigatus*. Biochem. Biophys. Res. Commun. 411, 549–554.
Ruiz-Herrera, J., Sing, V.O., Van der Woude, W.J., Bartnicki-García, S., 1975. Microfibril assembly by granules of chitin synthetase. Proc. Natl. Acad. Sci. USA 72, 2706–2710.
Sacher, M., Barrowman, J., Wang, W., Horecka, J., Zhang, Y., Pypaert, M., Ferro-Novick, S., 2001. TRAPP I implicated in the specificity of tethering in ER-to-Golgi transport. Mol. Cell 7, 433–442.
Sanchatjate, S., Schekman, R., 2006. Chs5/6 complex: a multiprotein complex that interacts with and conveys chitin synthase III from the trans-Golgi network to the cell surface. Mol. Biol. Cell 17, 4157–4166.
Sánchez-León, E., Verdin, J., Freitag, M., Roberson, R.W., Bartnicki-García, S., Riquelme, M., 2011. Traffic of chitin synthase 1 (CHS-1) to the Spitzenkorper and developing septa in hyphae of *Neurospora crassa*: actin dependence and evidence of distinct microvesicle populations. Eukaryot. Cell 10, 683–695.
Sánchez-León, E., Bowman, B., Seidel, C., Fischer, R., Novick, P., Riquelme, M., 2014. The Rab GTPase YPT-1 associates with Golgi cisternae and Spitzenkörper microvesicles in *Neurospora crassa*. Mol. Microbiol., in press. http://dx.doi.org/10.1111/mmi.12878.
Santos, B., Snyder, M., 1997. Targeting of chitin synthase 3 to polarized growth sites in yeast requires Chs5p and Myo2p. J. Cell Biol. 136, 95–110.
Sanz, M., Castrejon, F., Duran, A., Roncero, C., 2004. *Saccharomyces cerevisiae* Bni4p directs the formation of the chitin ring and also participates in the correct assembly of the septum structure. Microbiology 150, 3229–3241.
Scott, B., Eaton, C.J., 2008. Role of reactive oxygen species in fungal cellular differentiations. Curr. Opin. Microbiol. 11, 488–493.
Sentandreu, R., Martinez-Ramon, A., Ruiz-Herrera, J., 1984. Localization of chitin synthase in *Mucor rouxii* by an autoradiographic method. J. Genet. Microbiol. 130, 1193–1199.
Sha, B., Phillips, S.E., Bankaitis, V.A., Luo, M., 1998. Crystal structure of the *Saccharomyces cerevisiae* phosphatidylinositol-transfer protein. Nature 391, 506–510.
Shaw, J.A., Mol, P.C., Bowers, B., Silverman, S.J., Valdivieso, M.H., Duran, A., Cabib, E., 1991. The function of chitin synthases 2 and 3 in the *Saccharomyces cerevisiae* cell cycle. J. Cell Biol. 114, 111–123.
Sheng, W., Yamashita, S., Ohta, A., Horiuchi, H., 2013. Functional differentiation of chitin synthases in *Yarrowia lipolytica*. Biosci. Biotechnol. Biochem. 77, 1275–1281.
Silverman, S.J., Sburlati, A., Slater, M.L., Cabib, E., 1988. Chitin synthase 2 is essential for septum formation and cell division in *Saccharomyces cerevisiae*. Proc. Natl. Acad. Sci. USA 85, 4735–4739.
Soulie, M.C., Perino, C., Piffeteau, A., Choquer, M., Malfatti, P., Cimerman, A., Kunz, C., Boccara, M., Vidal-Cros, A., 2006. *Botrytis cinerea* virulence is drastically reduced after disruption of chitin synthase class III gene (Bcchs3a). Cell. Microbiol. 8, 1310–1321.
Specht, C.A., Liu, Y., Robbins, P.W., Bulawa, C.E., Iartchouk, N., Winter, K.R., Riggle, P.J., Rhodes, J.C., Dodge, C.L., Culp, D.W., et al., 1996. The chsD and chsE genes of *Aspergillus nidulans* and their roles in chitin synthesis. Fungal Genet. Biol. 20, 153–167.
Starr, T.L., Pagant, S., Wang, C.W., Schekman, R., 2012. Sorting signals that mediate traffic of chitin synthase III between the TGN/endosomes and to the plasma membrane in yeast. PLoS ONE 7, e46386.
Suvorova, E.S., Duden, R., Lupashin, V.V., 2002. The Sec34/Sec35p complex, a Ypt1p effector required for retrograde intra-Golgi trafficking, interacts with Golgi SNAREs and COPI vesicle coat proteins. J. Cell Biol. 157, 631–643.
Szewczyk, E., Nayak, T., Oakley, C.E., Edgerton, H., Xiong, Y., Taheri-Talesh, N., Osmani, S.A., Oakley, B.R., 2006. Fusion PCR and gene targeting in *Aspergillus nidulans*. Nat. Protoc. 1, 3111–3120.
Takeshita, N., Ohta, A., Horiuchi, H., 2002. CsmA, a gene encoding a class V chitin synthase with a myosin motor-like domain of *Aspergillus nidulans*, is translated as a single polypeptide and regulated in response to osmotic conditions. Biochem. Biophys. Res. Commun. 298, 103–109.
Takeshita, N., Ohta, A., Horiuchi, H., 2005. CsmA, a class V chitin synthase with a myosin motor-like domain, is localized through direct interaction with the actin cytoskeleton in *Aspergillus nidulans*. Mol. Biol. Cell 16, 1961–1970.
Takeshita, N., Yamashita, S., Ohta, A., Horiuchi, H., 2006. *Aspergillus nidulans* class V and VI chitin synthases CsmA and CsmB, each with a myosin motor-like domain, perform compensatory functions that are essential for hyphal tip growth. Mol. Microbiol. 59, 1380–1394.
Teh, E.M., Chai, C.C., Yeong, F.M., 2009. Retention of Chs2p in the ER requires N-terminal CDK1-phosphorylation sites. Cell Cycle 8, 2964–2974.
Trautwein, M., Schindler, C., Gauss, R., Dengjel, J., Hartmann, E.A.S., 2006. Arf1p, Chs5p and the ChAPs are required for export of specialized cargo from the Golgi. EMBO J. 25, 943–954.
Trilla, J.A., Durán, A.C.R., 1999. Chs7p, a new protein involved in the control of protein export from the endoplasmic reticulum that is specifically engaged in the regulation of chitin synthesis in *Saccharomyces cerevisiae*. J. Cell Biol. 145, 1153–1163.
Valdivieso, M.H., Mol, P.C., Shaw, J.A., Cabib, E., Durán, A., 1991. CAL1, a gene required for activity of chitin synthase 3 in *Saccharomyces cerevisiae*. J. Cell Biol. 114, 101–109.
Verdín, J., Bartnicki-García, S., Riquelme, M., 2009. Functional stratification of the Spitzenkörper of *Neurospora crassa*. Mol. Microbiol. 74, 1044–1053.
VerPlank, L., Li, R., 2005. Cell cycle-regulated trafficking of Chs2 controls actomyosin ring stability during cytokinesis. Mol. Biol. Cell 16, 2529–2543.
Vogel, H.J., 1956. A convenient growth medium for *Neurospora* (Medium N). Microb. Genet. Bull. 13, 42–43.
Wang, Z., Zheng, L., Liu, H., Wang, Q., Hauser, M., Kauffman, S., Becker, J.M., Szaniszlo, P.J., 2001. WdChs2p, a class I chitin synthase, together with WdChs3p (class III) contributes to virulence in *Wangiella (Exophiala) dermatitidis*. Infect. Immun. 69, 7517–7526.
Wang, C.W., Hamamoto, S., Orci, L., Schekman, R., 2006. Exomer: a coat complex for transport of select membrane proteins from the trans-Golgi network to the plasma membrane in yeast. J. Cell Biol. 174, 973–983.
Weber, I., Assmann, D., Thines, E., Steinberg, G., 2006. Polar localizing class V myosin chitin synthases are essential during early plant infection in the plant pathogenic fungus *Ustilago maydis*. Plant Cell 18, 225–242.
Wessels, J.G.H., 1986. Cell wall synthesis in apical hyphal growth. Int. Rev. Cytol. 104, 37–79.
Westergaard, M., Mitchell, H.K., 1947. *Neurospora* V. A synthetic medium favoring sexual reproduction. Am. J. Bot. 34, 573–577.
Xoconostle-Cazares, B., Specht, C.A., Robbins, P.W., Liu, Y., Leon, C., Ruiz-Herrera, J., 1997. Umchs5, a gene coding for a class IV chitin synthase in *Ustilago maydis*. Fungal Genet. Biol. 22, 199–208.
Yarden, O., Yanofsky, C., 1991. Chitin synthase 1 plays a major role in cell wall biogenesis in *Neurospora crassa*. Genes Dev. 5, 2420–2430.
Zhang, G., Kashimshetty, R., Ng, K.E., Tan, H.B., Yeong, F.M., 2006. Exit from mitosis triggers Chs2p transport from the endoplasmic reticulum to mother-daughter neck via the secretory pathway in budding yeast. J. Cell Biol. 174, 207–220.
Ziman, M., Chuang, J.S., Tsung, M., Hamamoto, S., Schekman, R., 1998. Chs6p-dependent anterograde transport of Chs3p from the chitosome to the plasma membrane in *Saccharomyces cerevisiae*. Mol. Biol. Cell 9, 1565–1576.